THE USE OF OPEN ACCESS SATELLITE DATA TO IDENTIFY WILDFIRE FUEL TYPES

March 2021

Fire and Emergency New Zealand Research Report Number 181

ISBN Number 978-1-92-728743-9
ISSN Number 2703-1705

Joy, K., Gerretzen, D., Kindred, M., & Soni, S. (2021). The use of open access satellite data to identify wildfire fuel types (Report No. 181). Orbica, Christchurch, NZ: Fire and Emergency New Zealand.

This research was commissioned by Fire and Emergency New Zealand and undertaken by independent researchers. Publication does not indicate Fire and Emergency New Zealand's endorsement of the findings or recommendations.

Fire and Emergency New Zealand

The use of open access satellite data to identify wildfire fuel types

DATE:
15 March 2021
Version 4.0 (Contains variation)
Kurt.joy@orbica.World

EXECUTIVE SUMMARY

This document reports on the findings of work undertaken by Orbica for Fire and Emergency New Zealand (FENZ), the key focus being to address the questions:

"Can open-access satellite imagery be used to augment current land use datasets? And if so, can this be used to regularly update wildfire fuel types?"

Sentinel-2 satellite data, collected and released by the European Space Agency, has 10 m ground resolution, 12 bands and a five-day revisit time. Given these characteristics and combined with computational machine learning algorithms, Sentinel-2 makes an excellent choice for this project. Using these techniques, several key wildfire fuel classes were tested to see if a Sentinel and machine learning approach could aid in the creation of updated datasets for: Urban expansion, hedgerows and shelter belts, broom/gorse, water bodies and exotic forestry.

Our work shows that with enough training data, and in settings where a medium scale spatial resolution is appropriate, data can be produced using a variety of semi and/or automated image segmentation tools. Using open-source software and programming libraries (i.e. free) extra value can be added to datasets such as the Landcare LCDB or LUCAS from the Ministry for the Environment. Taking such an approach allows datasets, with a typical five-year update time, to be updated on a far more regular basis, and down to five days if necessary. Only one of the assessments, that of forestry age, was deemed unsuitable for Sentinel-2. In this case LINZ aerial imagery, proved more effective when combined with CNN deep learning models.

The ability of these models to be automated was also considered. Several possible scenarios for semi/fully automated processing pipelines have been suggested for integration within the FENZ infrastructure. Options include: Timed release (i.e. quarterly) or on demand (i.e. ad-hoc processing, running on local or cloud computing). All these options depend on budget (5-200k NZD), delivery times and available hardware.

GLOSSARY

AI	Artificial Intelligence
AOI	Area of Interest
API	Application Programming Interface
CNN	Convolutional Neural Network
COH	Copernicus Open Access Hub
ECAN	Environment Canterbury
EO	Earth observation
ESA	European Space Agency
FCIR	False colour infrared
FENZ	Fire and Emergency New Zealand
GPU	Graphic Processing Unit
GSD	Ground Surface Distance
IOU	Intersection Over Union
L1A	Level 1, Top of Atmosphere calibration
L2C	Level 2, Bottom of Atmosphere calibration
LCDB	Land Cover Database
LINZ	Land Information New Zealand
LUCAS	Land Use and Carbon Analysis System
MS	Multi-spectral
MSI	Multi Spectral Imagery
NASA	National Administration and Space Agency
NDWI	Normalised Difference Wetness Index
NDVI	Normalised Difference Vegetation Index
NRT	Near Real time Tasking
NZD	New Zealand Dollars
QA	Quality Assessment
QC	Quality control
RS	Remote Sensing
RGB	Red, Green, Blue
S2	Sentinel-2
SAR	Synthetic aperture radar
SWIR	Shortwave Infrared
SVM	Support Vector Machines
TIR	Thermal infrared
USD	United States Dollars
USGS	United States Geological Survey
VISNIR	Visible / Near Infrared spectrum
WMS	Web mapping service
WFS	Web feature service
WV3	World View 3

CONTENTS

TABLE OF FIGURES

TABLE OF TABLES

1. PROJECT BACKGROUND AND SCOPE

As a proxy for vegetative fuel distribution throughout New Zealand, Fire and Emergency New Zealand (FENZ) use land cover vegetation datasets to support the assessment of wildfire risk around the country. Typically, this has been in the form of the Land Cover Database (LCDB) released by Landcare Research–Maanaki Whenua. Unfortunately, there are two underlying problems with the use of this dataset:

- Only periodically updated and is proving to be less reliable the older it is.
- With time, it has also evolved, and subclasses have been aggregated. This is particularly problematic in the case of exotic forestry where eight classes are now merged to a single class.

The use of such outdated or aggregated data reduces the accuracy of any wildfire risk assessment and thus FENZ cannot adequately assess this with a high level of certainty. With the work of Scion now identifying and modelling up to 50 discrete fuel types (pers comms), an annually updated land cover dataset aligned to the fuel types would provide FENZ with a far more up to date picture of vegetation fuel types and their associated fire potential.

Given the problem, Orbica was tasked with assessing:

- The changes in the various releases of the LCDB
- If the LCDB is still a valid output to use within fire modelling such as Prometheus and other risk/threat identification tools
- If the LCDB can be expanded to include further breakdown of the fuel classes, such as generating different forestry age classes and the separation of gorse and broom.

The following report prepared by Orbica evaluates the use of open-access satellite imagery with machine-learning techniques to identify various fuel classes. It is hoped that the successful automated identification of fuel classes will enable them to be used in annual updates to wildfire risk assessment, at least in terms of the fuel hazard. FENZ has identified five key fuel classes that are either spatially incorrect or are missing within the various LCDB datasets.

These fuel classes are:

- Exotic forest plantations
- Shelterbelts and hedgerows
- Gorse and broom scrub
- Urban area expansion
- Water bodies. Rivers, streams, lakes, and ponds.

2. SATELLITE IMAGERY CONSIDERATIONS

With all remote sensing (RS) projects that employ orbitally acquired data, five primary attributes drive the choice of imagery to be used. 1) Instrument choice, 2) temporal resolution, 3) spectral resolution, 4) spatial resolution and 5) acquisition cost.

Unfortunately, it is typically the latter that is the major limitation on the type of imagery employed in RS projects. The gold standard in satellite derived imagery is the multispectral imagery (MSI) from the Digital Globe/Maxar Worldview constellation, particularly Worldview 3 (WV3). Eight bands with a spatial resolution of 1.2 m can be pan-sharpened to 0.3 m daily, providing the highest quality imagery available. But this data comes with a price - near real time tasking (NRT) costs approximately $27 USD for 1 km^2 (minimum 100 km^2 per order).

Given the expense of the data, what other sources can be leveraged? ESA and USGS have long running Earth observation (EO) programmes in which the data is open access under creative commons licenses. Data from these are used widely in landscape change and water quality monitoring studies. With a spatial resolution of 15 m, 12 spectral bands, and an orbital revisit time of ~12 days, the latest generation (Landsat-8) continues a USGS EO programme that has been running since 1972. Although the Landsat data is well published in the literature, it is now being replaced with that from a European Space Agency (ESA) programme named Copernicus. As part of this programme several satellites with higher spatial resolution and shorter revisit times makes then more useful when considering time-based studies (Table 1).

Table 1: A list of USGS and ESA platforms that supply open access data. The type of onboard instrument or sensor is classified as multispectral (MS), synthetic aperture radar (SAR), thermal infrared (TIR) and spectrometer (SPEC). The final imagery requirement is the determining factor about what type of platform is employed for space-based observation.

Satellite / Platform	*Source*	*Date Range*	*Revisit Time*	*Sensor Type*	*Bands*	*Resolution*
LANDSAT 5	USGS	1984-2011	16 days	MS/TIR	6/1	60 m
LANDSAT 7	USGS	1999-2018	16 days	MS	7/1	15-60 m
LANDSAT 8	USGS	2013-	16 days	MS/TIR	9/2	15-100 m
LANDSAT 9	USGS	2020-	16 days	MS/TIR	9/2	15-100 m
SENTINEL 1A/B	ESA	2014/2016 -	6 days	SAR	N/A	9-93 m
SENTINEL 2A/B	ESA	2015/2017-	6 days	MS	12	10-60 m
SENTINEL 3A/B	ESA	2016/2018	6 days	SPEC	21	300-1200 m
SENTINEL 5P	ESA	2017-	16 days	SPEC	3	5500 m

While initially a commercial programme, in 2009 the United States Geological Survey (USGS) Landsat programme gave users free access to all data via its web portal (https://earthexplorer.usgs.gov/). In contrast, the ESA Copernicus program was built around a central tenet of open access data, either via the Copernicus Open Access Hub

(https://scihub.copernicus.eu/) or an application programming interface (API). When comparing such free imagery to that from commercial providers such as Maxar (i.e. Worldview), Airbus (i.e. Pleiades) and Planet (i.e. Rapid eye), the principal differences are 1) Surface resolution (i.e. ground surface distance or GSD), 2) revisit time and 3) tasking ability (Table 2). In most cases, commercial imagery has considerably higher spatial resolution, usually by several orders of magnitude, and has a sub-daily revisit time.

Table 2: Comparison between Sentinel-2 and commercial satellites. Archive cost is based on data being >90 days old. Additional <5% cloud free guarantee costs an extra 50%. 2019 Retail prices obtained from Landinfo (http://www.landinfo.com/satellite-imagery-pricing.html). Note that some platforms do not have a tasked pricing or a minimum required area.

Satellite / Platform	*Type (Band)*	*Cost per Km^2 (ARCHIVE/NRT/TASKED)*	*Maximum Resolution (px / m^2)*	*Revisit Time (Days)*	*Minimum Area (KM^2) (Archived/Tasked)*
SENTINEL-2	MSI (12)	Free	10	6	None
WORLDVIEW 1	(1)	$14 / $24 / $48	0.5	1	25km^2 /100km^2
WORLDVIEW 3	MSI (16)	$14 / $17 / $48	0.3	<1	25km^2 /100km^2
RAPIDEYE	MSI (5)	$1 / $6 / NA	5	1	500 km^2
PLEADIES-1	MSI (5)	$12 / $21 / $36	0.5	1	25km^2 /100km^2
IKONOS	MSI (5)	$10 / NA / $35	0.8	<3	25km^2 /100km^2

But for many tasks where a high temporal resolution is required, the ongoing costs associated with commercial imagery acquired daily or weekly can be crippling, particularly in a location like New Zealand, where the lack of cloud free days can be problematic. Therefore, to insure against the probability of cloudy images an additional 25-50% increase to acquisition may need to be applied to ensure that imagery will be under the 5% cloud threshold.

For example, an event occurs on a known date that needs to be analysed, therefore, imagery immediately prior to and post event within the NRT period must be purchased. Additionally, as the spatial extent of the event is relatively small, WV-3 imagery must be purchased with <5% cloud cover (Table 3).

Table 3: Example costing for a simple, prior/post RS task. Prices based on Landpro.com (4/13/2018)

Imagery prior to event:	$29 usd per km^2 (minimum 100km^2)	= $2900 usd
	<5% cloud cover guarantee	= $1450 usd
Imagery post event:	$29 usd per km^2 (minimum 100km^2)	= $2900 usd
	<5% cloud cover guarantee	= $1450 usd

Converting it from USD to NZD we get a cost of ~$13,000. An expensive exercise, even if treated as a worst-case scenario. Given this cost, it is easy to imagine organisations being extremely cautious in such an approach, thus the use of lower resolution imagery, even with their caveats, can be a powerful alternative.

Even with lower spatial and temporal resolution, the open access imagery of platforms such as Sentinel can provide a sandbox for testing and building RS solutions for land change monitoring that is de-risked compared to that of commercial imagery (Figure 1).

Figure 1: Example of commercial 0.6m Quickbird-2 (left) vs open access 10m Sentinel-2 (right) imagery for an area south of Whangamata in the Bay of Plenty. Approximately ten years separate the two images (QB-2 2009, S-2 2019).

If the target of interest is large enough and the period of identification (i.e. dates pre- and post-event) is coarse enough, such data is a viable solution even within a production environment. Therefore, for the purposes of this report, the use of Sentinel-2 imagery provides a perfect source of data to test: whether open access imagery can be used for vegetation classification? and is it a viable alternative to commercial imagery?

2.1. SENTINEL-2 MULTISPECTRAL IMAGERY (MSI)

Optical multispectral imagery (MSI) is a passive remote sensing technique and requires some form of illumination (i.e. the sun) to achieve results. Therefore, this data is not only constrained to daytime use but is also heavily affected by cloud cover. This is in stark contrast to the radar data acquired by the Sentinel-1 platform, in which actively emitted C-band microwaves self-illuminate a scene and clouds do not affect the data.

Multispectral imaging refers to the ability of an instrument to measure electromagnetic radiation outside of that visible by the human eye. The area of the electromagnetic spectrum (Figure 2) of interest in remote sensing applications is typically 350nm (blue) into 750nm (red), commonly referred to as visual range (i.e. radiation able to be seen by the naked eye). Beyond that, 750-2300 nm is infrared, which cannot be seen by eye but is absorbed by certain pigments and water.

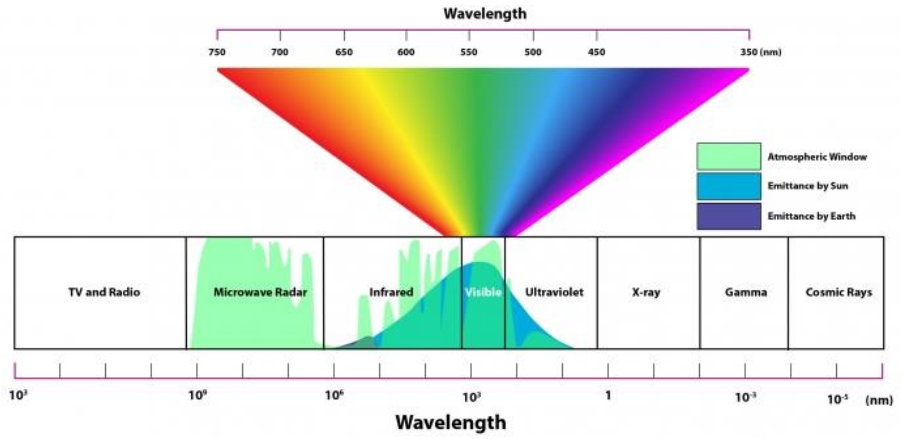

Figure 2: The electromagnetic spectrum. Light green regions in the lower panel show atmospheric windows and dark blue is the spectral response of the sun (image from Dutton Institute, Penn State).

Multispectral bands, or zones of measured radiation, are defined by wavelengths that can be transmitted though the atmosphere un-attenuated. This is especially pertinent to bands within the near infrared (NIR) range where they are heavily affected by atmospheric water vapour. Thus, the band selection of bands is relatively constrained for use for remote sensing applications and is similar between instruments on different orbital platforms.

2.1.1. SENTINEL-2 TECHNICAL DATA

The Sentinel-2A spacecraft was launched in June 2015, with its sister, Sentinel-2B, in orbit in 2017. The satellites are part of an optical imaging mission to collect global change datasets on vegetation, soil, and water. Additionally, the missions provide atmospheric absorption and distortion data corrections at high resolution to provide enhanced continuity of data so far provided by SPOT-5 and Landsat-7 platforms.

Given a global dataset focus, the revisit requirements for Sentinel-2 are better than or equal to seven days over all landmasses and inland waters. As with S1A and S1B, the paired satellites allow a considerably shorter revisit and both follow the same 100-minute orbit, but

180° apart. This allows maximum coverage, and each satellite collects ~149 million km^2 of imagery per orbit (approximately 1.6 Tb). Therefore, in a single day (~15 orbits), the Sentinel-2 spacecraft transmit ~50 Tb of raw data back to earth via a combination of dedicated ground stations and orbital relay satellites.

The primary instrumentation is a push broom type multispectral imager (MSI) featuring a swath of 285 km with 13 bands covering a spectral range of 442-2200 nm at a variety of resolutions (Table 4).

Table 4: Spectral bands available for Sentinel-2. Central wavelength is calculated as the mean of S2A and S2B instruments

Band	*Name*	*Central wavelength (nm)*	*Bandwidth (nm FWHM)*	*Resolution (m)*
1	Atmospheric correction (aerosols)	443	21	60x60
2	Blue	493	66	10x10
3	Green	560	36	10x10
4	Red	665	31	10x10
5	Red edge 1	704	15	20x20
6	Red edge 2	740	15	20x20
7	Red edge 3	783	22	20x20
8	NIR	833	106	10x10
8a	Red edge 4	865	21	20x20
9	Atmospheric correction (water)	944	20	60x60
10	Cirrus correction	1375	31	60x60
11	SWIR 1	1612	91	20x20
12	SWIR 2	2195	175	20x20

The lack of a true panchromatic band should be noted and may be a problem in applications where pan-sharpening is required. As only the main VISNIR bands (4, 3, 2 and 8) have the maximum resolution, one technique to bypass this limitation is to make a single band composite from any three of the higher resolution (10 m) bands and apply this as a sharpening filter (e.g. Gram Schmitt) to the lower resolution bands (20-60 m).

2.2. DATA DISSEMINATION AND ACCESS

2.2.1. COPERNICUS OPEN ACCESS HUB (COH)

Given the purpose of the Copernicus programme is to provide open data for Earth observation, the dissemination and analysis tools are a key component. As the data itself is open source, several third-party companies have emerged as data distributors, with their selling point being easier data access, via web services, or easier analytics, via APIs. The following discussion looks at the advantages and disadvantages of one such system, Synergises' Sentinel-hub (https://sentinel-hub.com/) versus the Copernicus open access hub.

2.2.2. SENTINEL HUB

A different approach to data access is provided by third party companies such as Sinergise. The Sinergise paradigm is that instead of end-users interacting with, and processing, raw data from ESA, users have access to curated global datasets. Sentinel-Hub (www.sentinel-hub.com) provides users a more simplistic way to view data, but also a fully featured python API with machine learning, data cube storage and analytic tools. Sentinel Hub is a paid service that has several tiers, that provide a range of processing units and access based on research / commercial use (Table 5).

Table 5: Pricing breakdown for Sentinel Hub as of February 2020 (https://sentinel-hub.com/pricing-plans)

	Get Started	*Individual (non-commercial)*	*Individual (commercial)*	*Enterprise (Basic)*	*Enterprise (Enlarged)*
Price	Free	~$277 nzd/yr	~$1700 nzd/yr	~$10000 nzd/yr	~$20000 nzd/yr
Raw data download	N	Y	Y	Y	Y
Web services	N	Y	Y	Y	Y
API	N	Y	Y	Y	Y
Rate limits (Requests per minute/ processing units per month)	NA	300/30k	500/50k	600/200k	600/500k
Non-Commercial use	Y	Y	Y	Y	Y
Number of users	1	1	1	∞	∞
Mobile apps	N	N	N	Y	Y

2.2.3. SERVICES

A key strength of the Sentinel Hub suite of tools is the ability to use rendered on the fly imagery. While the initial selection is limited, a user can import a range of pre-existing or their own custom spectral indices. Within Sentinel Hub, a configuration tool allows the creation of multiple instances, each with their own API key, that can include any number of Web mapping service (WMS) endpoints. Each of which contains a JavaScript configuration script that can be filtered by date and tile-level cloud cover. The custom configuration script also allows a user to define:

- Histogram stretching
- Visualisation type
- Symbology
- Band combination.

Sentinel Hub also provides several easy to access web-based tools. Sentinel playground and EO browser are the “Google Maps” of satellite data in the Sentinel-Hub world. Sentinel playground (https://sentinel-hub.com/explore/sentinel-playground) is the most simplistic and provides the user with a series of pre-processed data that can be explored. Filtering is basic, by date, location, and cloud cover, but playground gives instant access to a variety of global Sentinel-2 visualised data products (Figure 3).

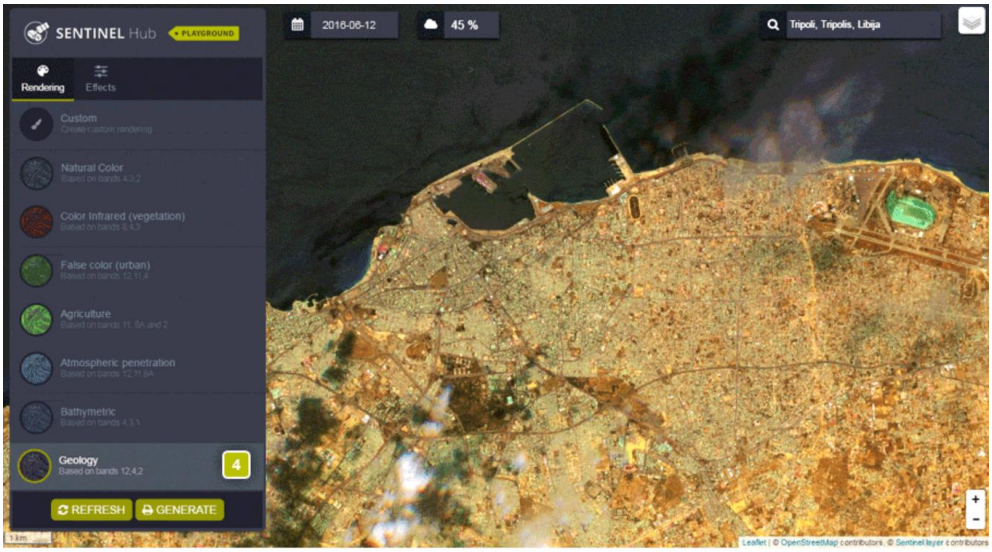

Figure 3: Sentinel Playground screen capture of Tripoli, Libya on the 12/6/2016. Data is a false colour (12, 4, 2) SWIR composite that highlights the regional geology.

EO-Brower is a more analytically focused product and requires a Sinergise account to access (Figure 4). As well as Sentinel platforms (S1, S2, S3 and S5P), several other freely accessible satellite datasets can be browsed and analysed (Table 6). Additionally, several other products, including the ASTER global elevation model, are available via the NASA Global Imagery Browser Service (GIBS, https://wiki.earthdata.nasa.gov/pages/viewpage.action?pageId=2228230).

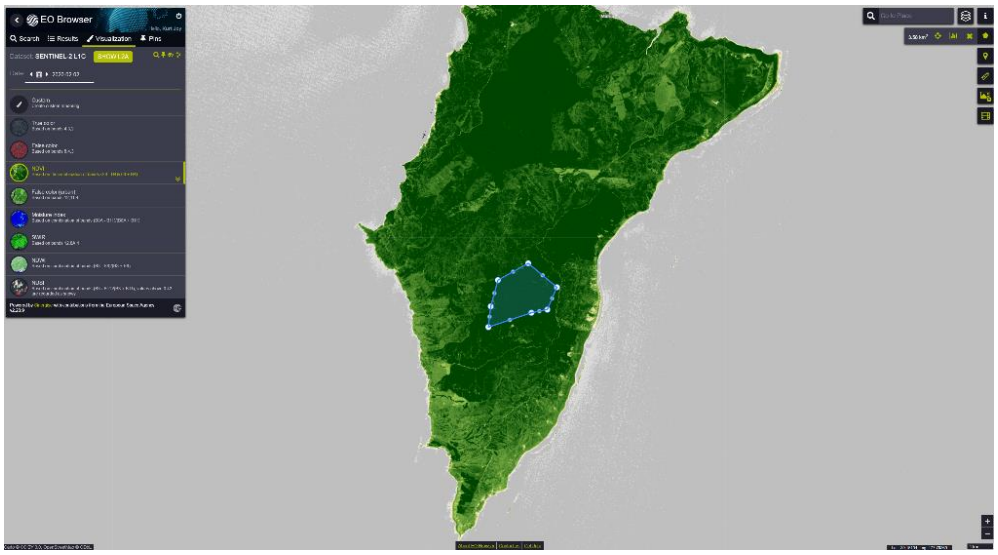

Figure 4: EO Browser showing NDVI for the Mahia Peninsular in Hawkes Bay.

Table 6: Additional open access datasets available via EO Browser.

Name	*Revisit*	*Resolution (Spatial)*	*Date range*	*Description*
LANDSAT (5,6,7,8)	16 days	0.003 – 0.1 km	1984-present	Multispectral including thermal. 4-11 bands (432-12100 nm)
MODIS	1-2 days	0.25-1 km	1999- present	Multispectral including thermal. 36 bands (400-15000 nm)
MERIS	3 days	0.25 km	2002-2012	Vegetation and ocean monitoring. 15 bands (290-1040 nm)
Proba-V	1-10 days	0.1, 0.33, 1 km	2001- present	Vegetation monitoring. Four bands (BLUE, RED, NIR, SWIR)

3. LANDCOVER DATABASE COMPARISON

A key dataset used in Prometheus and FENZs wildfire threat modelling is the NZ Land Cover Database (LCDB) produced by Landcare Research-Manaaki Whenua. It is a comprehensive land cover classification, grouping together similar land cover types based on satellite imagery into a shared taxonomy.

Several important updates have been made since the release of the dataset, particularly versions 2 (2002) and 5 (2020). Although version 5 is the most up to date and provides the most accurate picture of a real vegetation cover, the decision was made to integrate and merge several subclasses in later releases (Table 7).

This has led to a situation where the most up to date dataset in a spatial context (v5 in 2020) does not contain the required resolution in discrete land classes. The trade-off for having more detailed land cover classes is that data is out of data by ~18 years, increasing the ambiguity of the fuel types which therefore reduces the ability to accurately model fire damage potential.

FENZ have been primarily using LCDB2 as inputs into their threat assessment model, due to the higher resolution of land classes, and thus possible wildfire fuel types. But the acknowledged “elephant” in the room is the age and thus validity of the data’s spatial extent. Although version 5 is recognised as being more up to date, the merging of subclasses, particularly in the “Exotic forestry” class is a stumbling block to the adoption of LCDB5.

Table 7: A comparison of LCDB class codes between versions 2 and 4

	LCDB V2		LCDB V4 AND ONWARD	
	Class Code	***Class Name***	***Class Code***	***Class Name***
OTHER			0	Not land (used in V5 onwards)
ARTIFICIAL SURFACES	1	Built up area (Settlement)	1	Built up area (Settlement)
	2	Urban parkland / Open space	2	Urban parkland / Open space
	3	Surface mine	6	Surface mines and dumps
	4	Dump		
	5	Transportation infrastructure	5	Transportation infrastructure
BARE OR LIGHTLY VEGETATED SURFACES	10	Coastal sand and gravel	10	Sand and gravel
	11	River and lakeshore gravel and rock	16	Gravel and rock
	13	Alpine gravel and rock		
	12	Landslide	12	Landslide
	14	Permanent snow and ice	14	Permanent snow and ice
	15	Alpine grass/herb field	15	Alpine grass/herb field
WATER BODIES	20	Lake and pond	20	Lake and pond
	21	River	21	River
	22	Estuarine open water	22	Estuarine open water
CROPLAND	30	Short-rotation cropland	30	Short-rotation cropland
	31	Vineyard	33	Orchard, vineyard, and other perennial crops
	32	Orchard and other perennial crops		
GRASSLAND, SEDGELAND, AND MARSHLAND	40	High producing exotic grassland	40	High producing exotic grassland
	41	Low producing grassland	41	Low producing grassland
	42	Tall tussock grassland	42	Tall tussock grassland
	44	Depleted grassland	44	Depleted grassland
	45	Herbaceous freshwater vegetation	45	Herbaceous freshwater vegetation
	46	Herbaceous saline vegetation	46	Herbaceous saline vegetation
	47	Flaxland	47	Flaxland
SCRUB AND SHRUBLANDS	50	Fern land	50	fenland
	51	Gorse and/or Broom	51	Gorse and/or Broom
	52	Manuka and/or Kanuka	52	Manuka and/or Kanuka
	53	Matagouri	58	Matagouri and/or grey scrub
	57	Grey scrub		
	54	Broadleaf indigenous hardwoods	54	Broadleaf indigenous hardwoods
	55	Sub-alpine shrubland	55	Sub-alpine shrubland
	56	Mixed-exotic shrubland	56	Mixed-exotic shrubland
	55	Peat shrubland (Chatham Island only)	80	Peat shrubland (Chatham Island only)
	56	Dune shrubland (Chatham Island only)	81	Dune shrubland (Chatham Island only)
FOREST	60	Minor shelterbelts	71	Exotic forests
	61	Major shelterbelts		
	62	Afforestation (not imaged)		
	63	Afforestation (imaged post-lcdb1)		
	65	Pine forest – open canopy		
	66	Pine forest – closed canopy		
	67	Other exotic forest		
	64	Forest – harvested	64	Forest – harvested
	68	Deciduous hardwoods	68	Deciduous hardwoods
	69	Indigenous forest	69	Indigenous forest
	70	Mangrove	70	Mangrove

3.1. AREA CHANGE COMPARISONS

Quantifying the changes between LCDB2 and LCDB5 is key to understanding the net gain and loss in classified land area. Those classes that have undergone aggregation between the different LCDB versions are especially important, as the overall areal change in a class may be caused by the reorganisation of classes and not change of area. Thus, to gauge the overall change in classified land area, the focus of the following section is on those classes which have significant change in Table 8.

Table 8: Top ten classes with changes to land area by classification across New Zealand from LCDB2 to LCDB5

LCDB class name	*LCDB2 area (ha)*	*LCDB5 area (ha)*	*Area Change (ha)*	*Percentage Change (v2 to v5)*
High Producing Exotic Grassland	8,892,102	8,684,362	-207,740	-2%
Indigenous Forest	6,463,806	6,307,010	-156,796	-2%
Broadleaved Indigenous Hardwoods	540,009	696,531	156,522	3%
Low Producing Grassland	1,653,145	1,754,076	100,930	1%
Exotic Forest	1,741,475	1,838,310	96,835	1%
Depleted Tussock Grassland	250,608	169,501	-81,107	-3%
Tall Tussock Grassland	2,397,576	2,335,410	-62,166	-0.5%
Sub Alpine Shrubland	385,658	432,966	47,308	1%
Herbaceous Freshwater Vegetation	88,782	129,097	40,315	5%
Forest Harvested	234,943	199,483	-35,460	-2%

Given these changes, land classes with the highest variability have been investigated to understand what land class changes have occurred in the nearly two-decade period between the two LCDB releases, and what the class has changed from/to. It should be noted that land changes between two very different classes are more likely to be actual land changes, such as grasslands or trees, in contrast to those land changes within the same class. This change could also be interpreted as a change in the methodology used to calculate land cover classes.

3.1.1. GREATEST ABSOLUTE CHANGE IN AREA

"High Producing Exotic Grassland" has seen the greatest decrease with a change of 207,740 ha from LCDB2 to LCDB5, with approximately half attributed to a switch to the "Exotic Forest" class (Figure 5). Interestingly, almost 20% has remained as productive land and has been converted into cropland with a further 10% being converted into built up or urban land. A possible reason for the latter is the expansion of urban margins into the relatively clear surrounding rural margins.

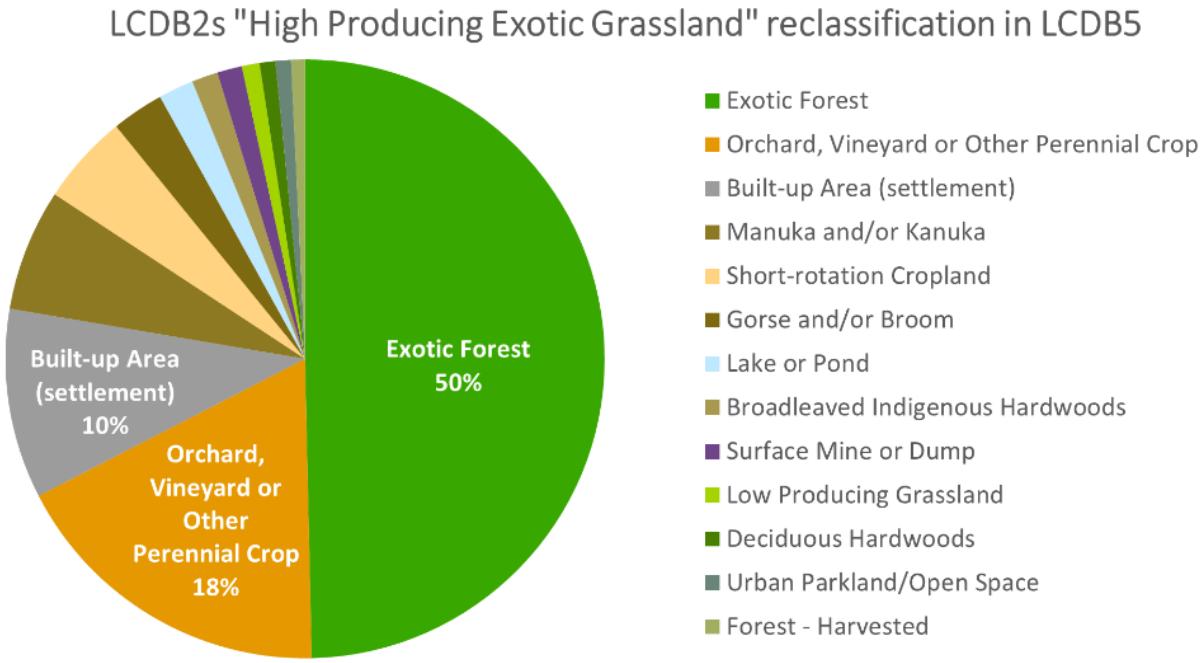

Figure 5: The primary classes that High Producing Exotic Grassland in 2001 has become in 2018.

The class with the greatest increase is "Broadleaved Indigenous Hardwoods" which has increased 156,522 ha from LCDB2 to LCDB5. Two thirds of this value were previously classified as "Manuka and/or Kanuka" and "Exotic Forest" in LCDB2 (Figure 6). This may be a result of a combination of either forest-to-forest conversion or a change in the algorithm used to calculate land cover classes. One fifth was high and low producing grassland in LCDB2. This is likely to be from landowners planting or allowing reversion to indigenous species to occur.

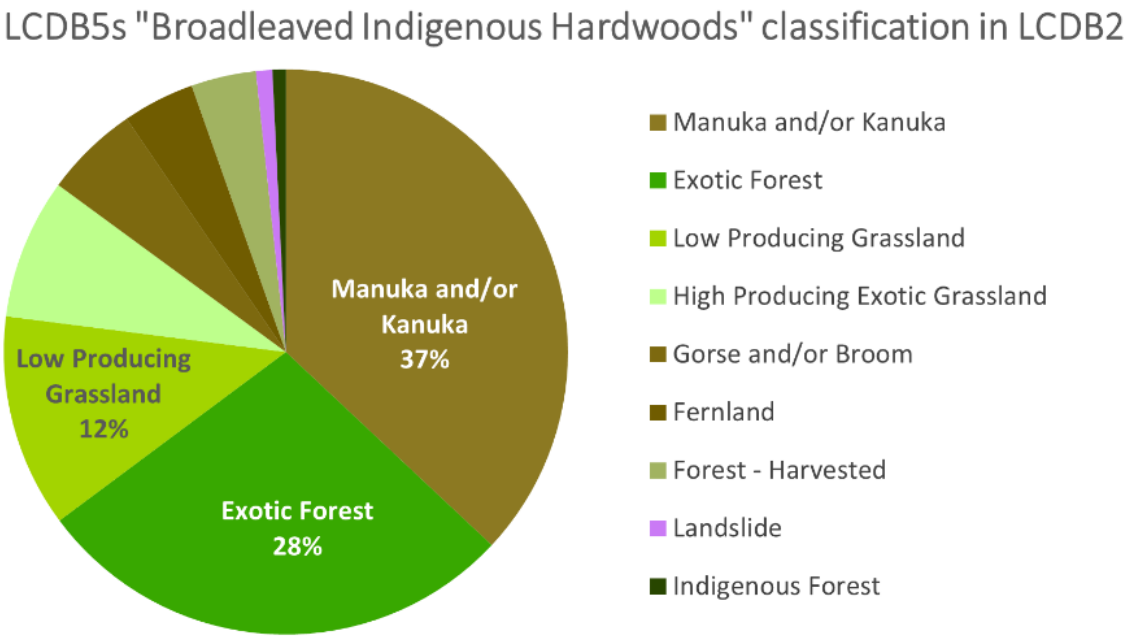

Figure 6: Chart shows what Broadleaved Indigenous Hardwoods in 2018 were in 2001, excluding Broadleaved Indigenous Hardwoods

3.1.2. GREATEST RELATIVE CHANGE IN AREA

The greatest relative decrease in area has occurred within the “Depleted Grassland” class which has decreased 3% or 81,107 ha from LCDB2 to LCDB5. Almost 90% remains as grassland although has been reclassified as either low or high producing (Figure 7). A likely explanation for this change may be due to landowners improving grass quality or a change in the algorithm used to calculate land cover classes.

“Herbaceous Freshwater Vegetation” is the class with greatest relative increase in area, with an increase of 5%, or 40,315 ha) from LCDB2 to LCDB5 (Figure 8). Half of this increase came from land previously classified as Deciduous Hardwoods, with much of the remaining area previously classed as grassland or lake/pond. The change in area is likely the result of land being reverted or converted to wetlands and water drainage areas.

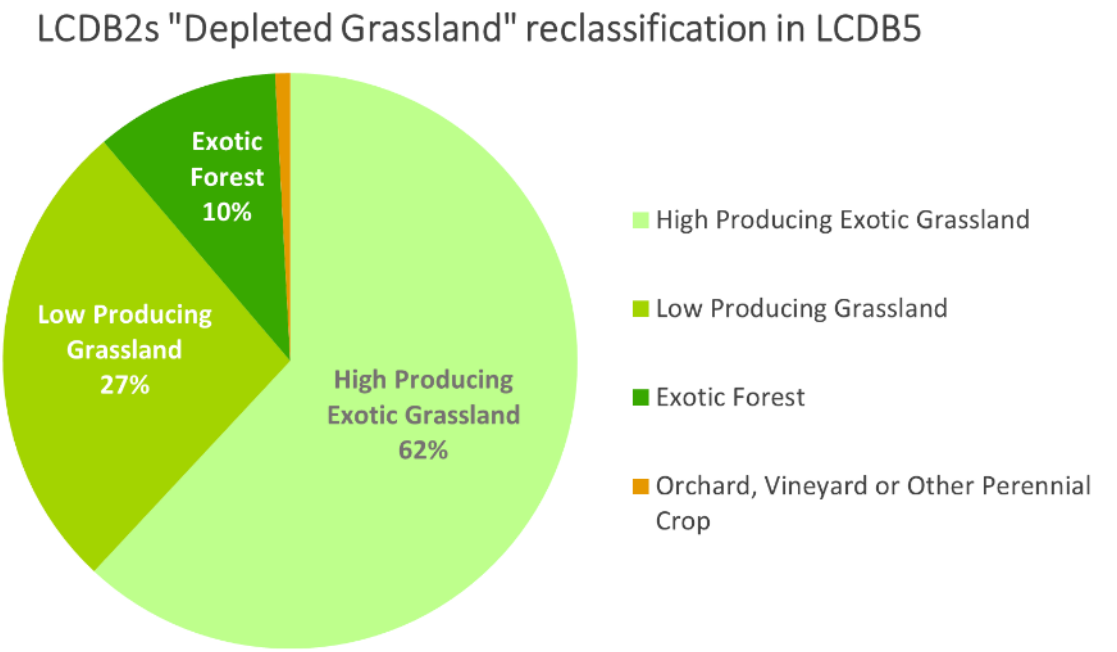

Figure 7: Depleted Grasslands conversion from 2001 to 2018.

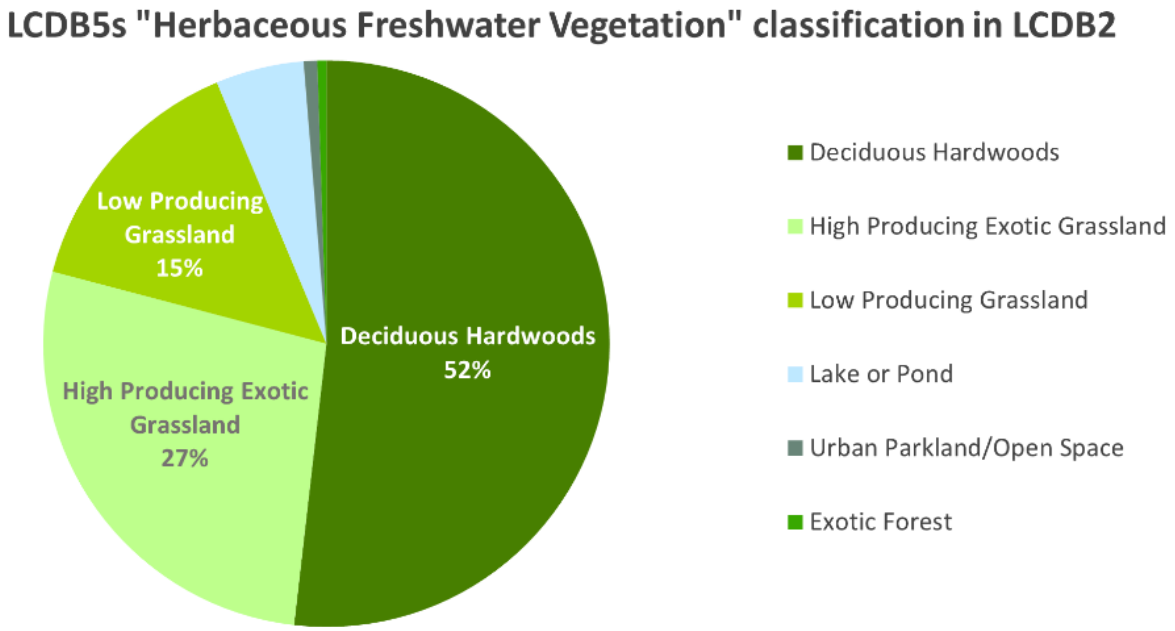

Figure 8: Herbaceous Freshwater Vegetation conversion from 2001 to 2018, excluding Herbaceous Freshwater Vegetation

4. CASE STUDY 1: EXOTIC FORESTRY

FENZ are currently using the forest classifications from LCDB to identify exotic forest. Unfortunately, in a review post 2002, a number of these classes were merged in later releases of the LCDB, resulting in a broader, and less useful classification to FENZ. Additionally, the review did not appear to address some errors in the classification method.

The LCDB is only updated every five years whereas the forest industry is extremely dynamic and changes to vegetation and landscape can occur daily. To keep up with these rapid changes, annually updated forest classifications are far better suited to reflect the current state of the environment in the forestry sector. Therefore, to aid the classification of exotic forestry, Sentinel-2 satellite imagery has been used in conjunction with machine learning techniques to separate exotic from native afforestation.

As previously stated, a key change in the classification system of "Forest" between LCDB2 to LCDB5 is the removal/aggregation of the underlying subunits, in particular the "Shelterbelts" and "Planted forest" sub-classifications. The effect of this aggregation has led to the classification becoming less detailed, as the seven classes used in LCDB2 (classes 60-67 excluding 64) have been combined into class 71 in LCDB5 (Table 9).

Table 9: Forest sub-classes in LCDB2 (2nd and 3rd columns) and LCDB4 to 5 (4th and 5th columns).

	LCDB V2		*LCDB V4 AND ONWARD*	
	Class Code	*Class Name*	*Class Code*	*Class Name*
FOREST	60	Minor shelterbelts	71	Exotic forests
	61	Major shelterbelts		
	62	Afforestation (not imaged)		
	63	Afforestation (imaged post-lcdb1)		
	65	Pine forest – open canopy		
	66	Pine forest – closed canopy		
	67	Other exotic forest		
	64	Forest – harvested	64	Forest – harvested

To investigate the simplification of forestry classifications between the various LCDB releases, a representative study area is shown in Figure 9.

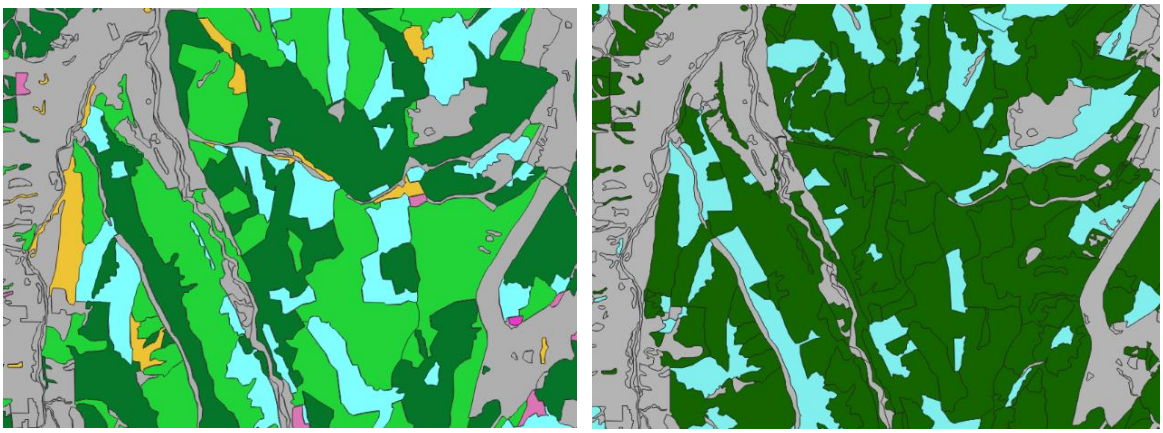

Figure 9: LCDB2 (left) showing forestry sub-classes – light green: open canopy pine, dark green: closed canopy pine, yellow: other exotic forest, pink: afforested varieties. LCDB5 (right) showing the exotic forestry class. Blue represents harvested areas in both.

On first comparison, it is clear the delineation of different forestry fuel classes has been lost, but the overall extent of forestry has undergone little change. As a result, there will be a negative impact on the ability to determine fire behaviour in the different forestry fuel classes. The blue areas identified as harvested are accurately represented when compared with aerial imagery.

The Ministry for the Environment's Land-use and Carbon Analysis System (LUCAS) 2016 Forest classification also shows similar forest extents. Unfortunately, LUCAS only identifies forestry as pre-1990 or post-1989 and does not identify harvested areas.

As well as issues surrounding the aggregation of classes, there are also occurrences of legacy errors in classification methodology that persist through multiple revisions of the LCDB.

Observed throughout the datasets, there are cases where algorithms used to calculate classes are not correctly identifying forestry. For example, there are parcels that were identified as "Exotic Forest" in LCDB2 and remain as such in LCDB5, yet they were not visible as exotic forest in 2018. This appears to be a legacy issue where at one point in time, the land may have been correctly, or incorrectly, classified as exotic forest and in later iterations the algorithm has not picked up on land use change, yet the classification remains. An example of this is shown below in Figure 10, where the two pink highlighted parcels are defined as Exotic Forest in LCDB5, but the underlying imagery from 2018 shows no forestry.

Figure 10: LCDB5 "Exotic Forest" parcels (left) overlaid on 2018 aerial imagery (right)

4.1. COLOUR SHIFTING CLASSIFICATION

Often the consistency and quality of colours in satellite imagery can vary depending on the location and time of year they were captured. Typically, sensor calibration is an important part of a postprocessing workflow to produce images that are matched in absolute reflectance values, colour, and gamma (brightness). In some cases, the ability to modify and exaggerate the colour of an image can be an extremely powerful technique in isolating or highlighting different features or classes.

In Sentinel-Hub (Section 2.2.2) colour properties can be adjusted to suit the users' needs. By increasing the gain, or brightness, the image becomes saturated and results in amplified colours. For forestry, the level of green shown in the image is of most interest as well as the influence of red and blue bands. Figure 11 shows an area of mixed native and exotic forestry and the effects of increasing image gain (brightness) and the strength of the red and blue channels. With an aim to isolate native from exotic vegetation, the right panel of Figure 11 below shows that an optimal colour would increase the gain while reducing the strength of the red and blue bands.

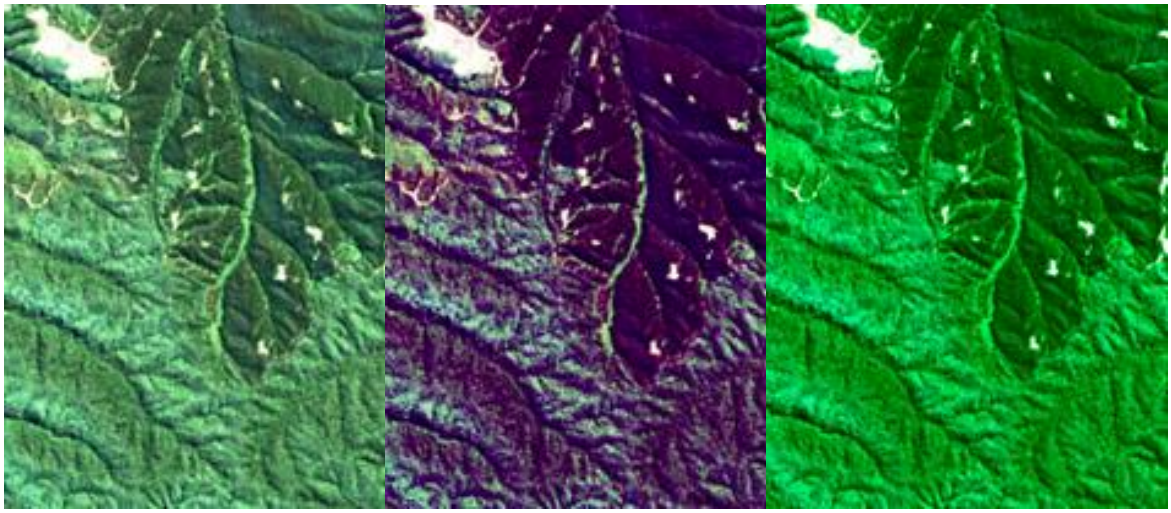

Figure 11: The effects of altering image gain on forested areas. High gain (left), medium to high gain (middle), and high gain with low red and blue values (right).

4.2. DEEP LEARNING CLASSIFICATION

To trial an artificial intelligence approach to image classification and segmentation, a commercially planted exotic forest area in Tasman has been selected. Spatial data of forestry stands provided by Onefortyone (https://onefortyone.com/) is for an AOI that contains a mix of ages within an active plantation initially established in 1936. The current crop is second or third rotation (Figure 12).

Figure 12: The Golden Downs study area identified by Onefortyone that contains a mix of species and rotations.

The data provided by Onefortyone defines several stands with obvious boundary lines of exotic forestry in proximity to native regeneration. To create training data for an AI analysis, the establishment date attribute field was used to code each stand into four main groups.

- Type 1: Exotic vegetation 1936 to 1974.
- Type 2: Non-exotic gully vegetation.
- Type 3: Exotic stand planted 2006 to 2010.
- Type 4: Exotic stand planted post 2011 to 2014.

4.3. AERIAL IMAGERY

The imagery we initially trialled was the 0.3 m Rural Aerial Photos (2016-2017) from Land Information New Zealand. The left side of Figure 13 shows the simplified Onefortyone plantation data with scrub and skids removed, and the right side with the final training dataset. The training data contained older exotic plantations (1936-1974 Type 1) and forests planted post 2006-2010 (Type 3), the latter comprising the majority of the AOI. Some classes were not included, these being the newly established Type 4 (cleared in 2014) and the gullies between plantations, likely a mix of native species (Type 2). To increase the training data within the area, Type 3 data was expanded in the area to the southeast.

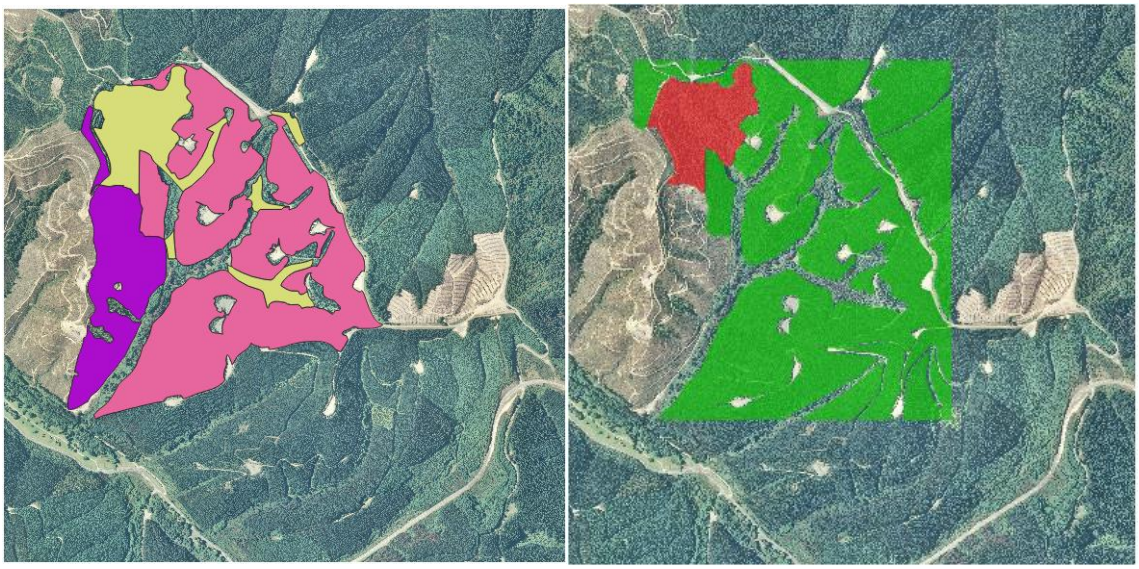

Figure 13: (Left) Training data supplied by Onefortyone from oldest to youngest: Type 1 (1937-1974, Yellow), Type 3 (2006-2010 Pink) and type 4 (2011-2014 Purple).
(Right) Two class expanded training data comprised of older (red) and younger-middle aged exotic plantations (green). Note that the remaining 5 km^2 of the AOI is used for model testing.

The deep learning AI model uses a convolutional neural network algorithm (CNN) to classify into

- Old growth exotic forestry (i.e. Type 1)
- Young or mid rotation exotic forestry (i.e. Type 3).

The preliminary results using the LINZ high resolution aerial imagery are shown in Figure 14.

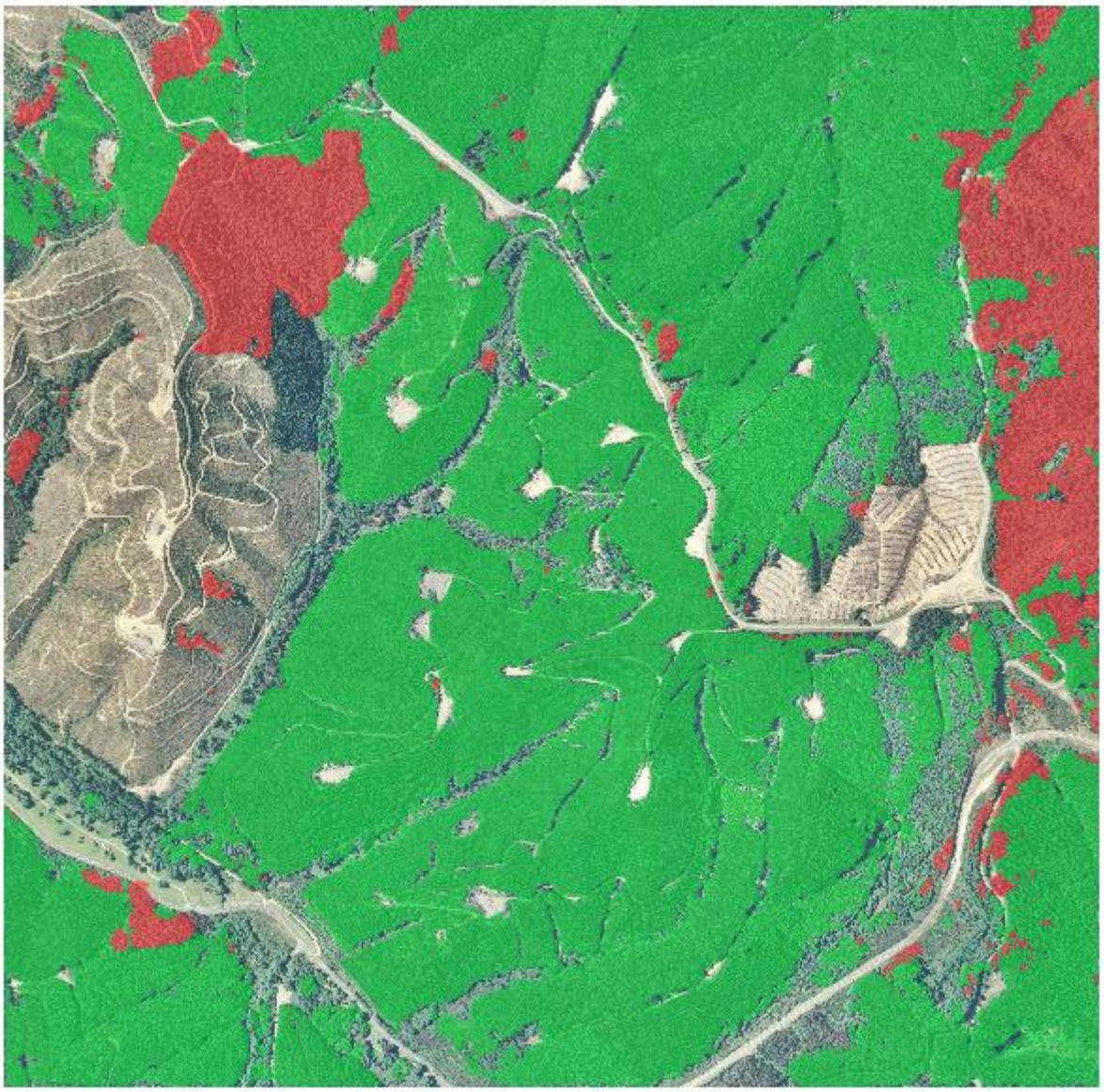

Figure 14: The two-class model prediction for the AOI shown in Figure 13. Red areas are older (1937-1974) and green areas represent younger exotic planting (2006 – 2010).

Overall, the model has done a good job at picking up concentrated areas of each classification but requires additional training and post processing to address the variegation and between native and exotic. A summary of the results (Table 10) shows a training IOU

(intersection over union) accuracy of ~93%, and a final visual QA of the results by a human analyst suggest a final testing accuracy of 85%.

Table 10: Model run times and IOU accuracy scores.

	Training	*Validation*	*Testing*
Number of images used	1 (1500 smaller patches)	1 (340 smaller patches)	1 (5000 smaller patches)
Time in minutes	120 min	1 min	2 min
Model loss (Error Rate %)	0.0128	0.0138	
Accuracy (IOU)	0.9345	0.9073	0.85 (QA/QC)

Given the limited amount of training data (one tile), the CNN model did extremely well in identifying native vs exotic forests within the AOI. The ability of CNN to incorporate the context of the training pixels (i.e. shape, texture, colour variation) to learn from shows the strength of the technique in this application.

4.4. SENTINEL IMAGERY

The use of the LINZ imagery combined with CNN algorithms proved that identifying forestry classes, and possibly age, can be achieved using high resolution imagery. Unfortunately, this may not be realistically achievable using Sentinel satellite data, due to its significantly lower resolution. To additionally test this hypothesis, several Sentinel-2 raw and derived data products acquired on 17/08/2019 were also tested using the same training AOI.

The Normalised Difference Vegetation Index (NDVI) is a spectral index that employs Sentinel-2 very near infrared (B8) and red (B4) bands.

$$NDVI = \frac{\left(NIR_{(B8)} - RED_{(B4)}\right)}{\left(NIR_{(B8)} + RED_{(B4)}\right)}$$

The NDVI shows the relative reflectance of chlorophyll absorption and is sensitive to variations in both chlorophyll concentrations and leaf area. Therefore, it provides a plant health metric that is generally unaffected by illumination variations and soil effects.

As shown in Figure 15, the AOI of forestry, supplied by Onefortyone and used in the previous examples, shows brighter values (heathier vegetation) in the younger exotic plantings (Figure 15, right bottom) and darker values in the older exotic vegetation (Figure 15, right top).

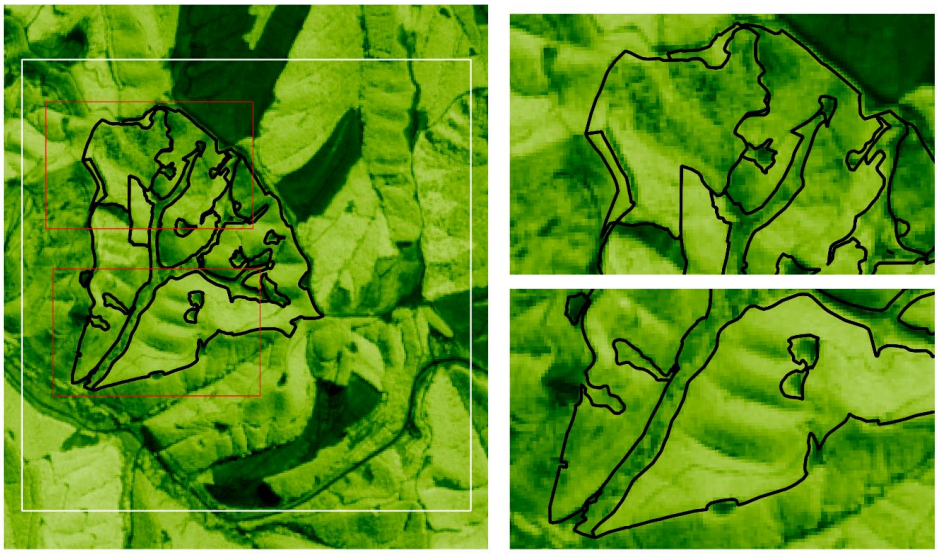

Figure 15: (Left) Normalised Difference Vegetation Index (NDVI) of the AOI (white box) overlain with the Onefortyone training data (Black). Side panels show areas of old-growth (Right top) and younger (right bottom) exotic forestry. Darker colours show less healthy vegetation and bare ground, and the lighter the reverse.

In this technique, instead of calculating an index using a combination of bands, the visualised bands are swapped around. So instead of a true colour representation of the data where:

$$RGB = R_{(B4)}\ G_{(B3)}\ B_{(B2)}$$

Bands are swapped around, and an infrared band is included. So that the red band colour is replaced with NIR, green with red, and blue with green.

$$FCIR = R_{(B8)}\ G_{(B4)}\ B_{(B3)}$$

The advantage of this technique is that it can highlight the spectral difference within an AOI and thus aid in the interpretation of complex imagery. As with the NDVI technique, False-colour infrared (FCIR) for the area (Figure 16) shows only minor visual changes between type 1 and type 2 forestry. This lack of differentiation between bands is also observed in the true colour imagery (Figure 17), where shadowing may play a role.

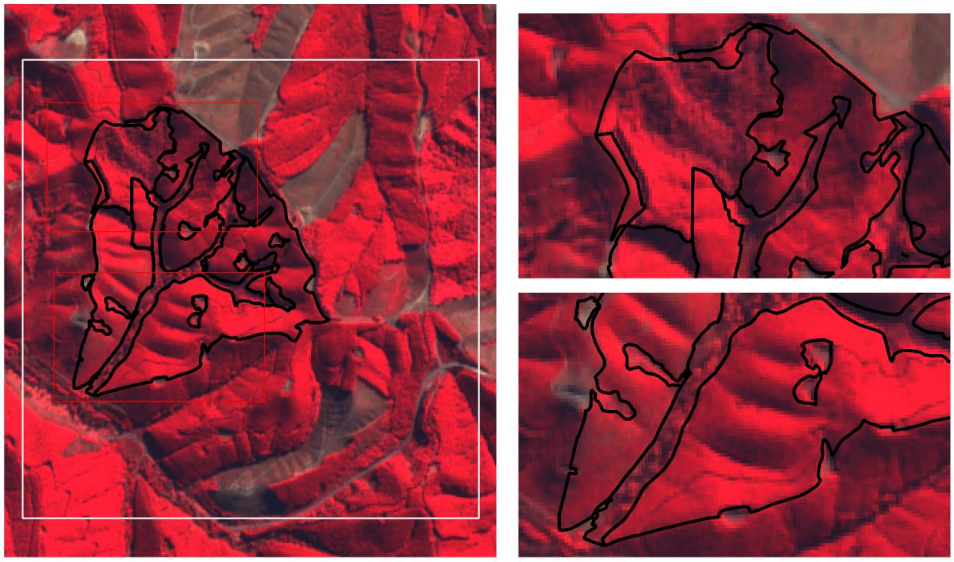

Figure 16: (Left) False-colour infrared (FCIR) of the AOI (white box) overlain with the Onefortyone training data (Black). Side panels show areas of old-growth (right top) and younger (right bottom) exotic forestry.

Figure 17: (Left) True colour (RGB) of the AOI (white box) overlain with the Onefortyone training data (Black). Side panels show areas of old-growth (right top) and younger (right bottom) exotic forestry.

Given the lack of pixel resolution in the Sentinel-2 imagery (10-60 m) compared to that of the LINZ 0.03 m imagery and the lack of differentiation between the various band combinations presented above, can machine learning techniques be employed?

Unsupervised K-means clustering was assessed as a method to group the pixel values into discrete units. Unfortunately, the use of CNN requires far more training data for use with the Sentinel imagery. The provided AOI is approximately 15000 Sentinel-2 pixels compared to the 17 million LINZ aerial pixels found in the same extent. These values mean that the same

CNN algorithm has orders of magnitude less pixels to learn off, which in the context of shape and texture can radically reduce the efficiency of the model.

The technique was applied to the NDVI, FCIR, and RGB true colour imagery (Figures 15, 16 and 17 above) to generate 4-5 clusters or groups of similar pixel values. Our results show that true colour RGB imagery, and NDVI produced the most successful clustering out of the various multi and single band layers respectively, the result of which is shown in Figures 18 and 19.

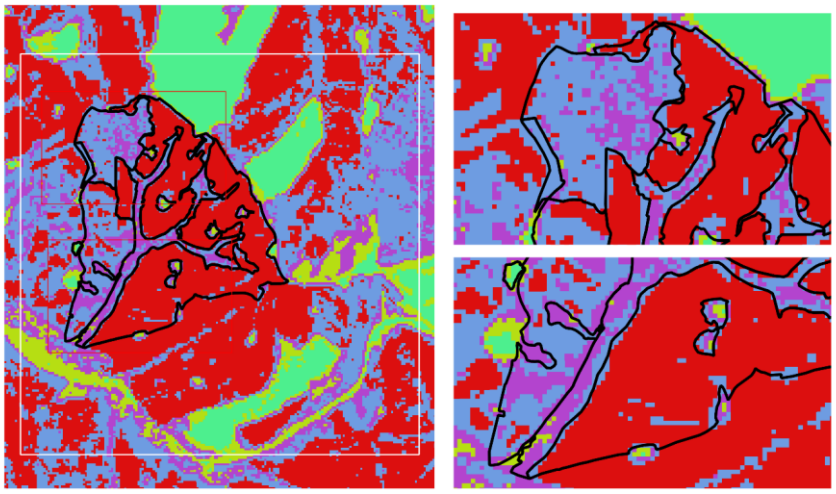

Figure 18: K means clustering (n=5) on single band Sentinel NDVI

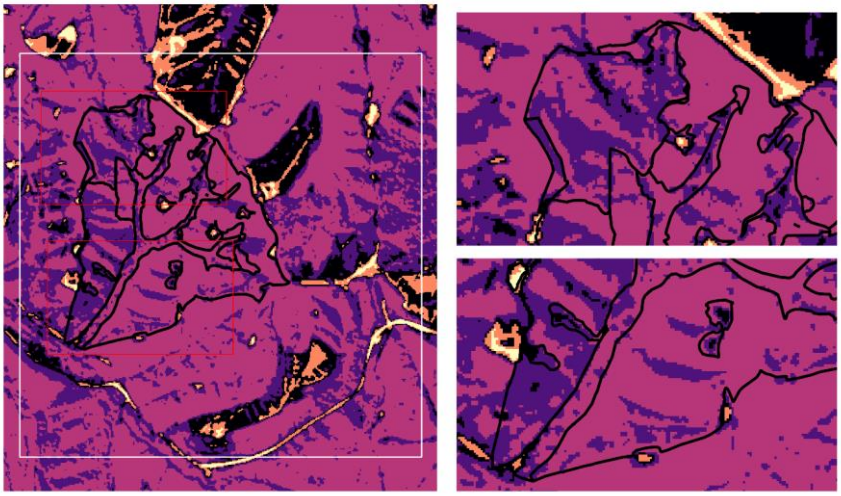

Figure 19: K means clustering (n=5) on multiband Sentinel RGB

As seen from the result shown in the above Figures, K-means clustering produced mixed results within the training area. The single band NDVI data (with values from -1 to +1), when clustered into five groups shows some good classification between various species. It does a good job of separating exotics to the east and south of the training data polygon, and additionally classifies both the older stand and the gully vegetation as indigenous. Unfortunately, it also misclassifies the exotic planting to the west of the image as indigenous species. This is in stark contrast to the true colour imagery. When the three colour bands (R,

G and B, all with 8-bit values from 0-255) are clustered into four groups, the K means method performs badly within the training area. Basically, classifying into slope aspect and shadowing (Figure 19 above).

Overall, the use of machine learning, and geostatistical techniques do show promise in the detection of indigenous vs native forestry, and possibly the age of exotic forestry. Although the above is a simple example of machine learning, and supplied only with a limited training dataset, it demonstrates the power of such algorithms applied to satellite imagery.

Colour shifting to enhance specific regions of greenness, appears to be a useful tool in separating, albeit qualitatively, tree species in homogenous plantations or stands. In contrast the use of CNN deep learning techniques, is particularly powerful and even a relatively small training dataset can be used on high resolution imagery to produce mapping of stands at the >80% level.

Unfortunately, training data with far larger extents are required to apply deep learning techniques to sentinel imagery, and the alternative, K-means clustering, modelled clusters relatively poorly compared to the CNN results.

To increase the accuracy and to assist with model training for afforested exotic forest and exotic forest blocks of different ages several additional points can be considered.

- The data supplied by Onefortyone was extremely valuable, and therefore it would be extremely beneficial to have more of these areas identified by forestry companies. These data, when used as model inputs, are precise and validated, eliminating assumptions made when selecting forest for different classifications. As expected, to leverage the maximum amount of value from such data, it would need to overlap with the acquisition of the imagery to effectively train the model. It is likely forestry data would only be required for the initial training of the model and not required on an ongoing basis, except when the model requires tuning.
- The inclusion of additional bands of satellite imagery. While the use of Sentinel-2 imagery in this report has typically been limited to true colour (3 band) imagery, 14 bands of various wavelength are available to be used.

5. CASE STUDY 2: SHELTERBELT DETECTION

Shelterbelts (e.g. windbreaks or hedgerows) are important infrastructure on farms across New Zealand as they provide protection from the elements to livestock and agricultural crops. Typically comprised of exotic species such as radiata pine or macrocarpa, they can form a barrier up to 15 m tall, a few metres wide and can span along fence lines for hundreds of metres. As such, shelterbelts create continuous fuel pathways which provide corridors for fire spread. They allow fire to travel in a direct path, ultimately enabling the fire to spread significant distances across areas where otherwise the dominant fuel type may be a limiting factor in terms of being less receptive to fire spread.

The primary challenge with detecting shelterbelts from satellite imagery is due to the nature of their geometry and size. With the pixel size of Sentinel-2 satellite imagery (Section 2.1) being 10 x 10 m (100 m^2), and the typical shelterbelt width being less than this, resolving such features can be problematic. Yet it is possible to train Artificial Intelligence (AI) algorithms to identify the dark green linear appearance of shelterbelts and windbreaks.

Using Sentinel-2 imagery, AI feature identification was applied to automatically identify and extract shelterbelts and windbreaks in Canterbury. The AOI being 15 km^2 of high producing grassland in the Rolleston / West Melton region that contains ~16 km of planted shelterbelts (Figure 20 Left). Sentinel-2 data was downloaded from ESA and processed within the Python API to create average summer cloud free true colour imagery for the AOI.

A convolutional neural network (CNN) deep learning architecture was developed that uses object-based image analysis. This type of AI feature segmentation identifies an object using not only the per-pixel RGB values found within a training area, but also the shape, geometry, and context of pixels within the image. As with all the techniques discussed here, training data was produced, initially as vector polygons, and then converted to the binary raster that the model will use to mask out the features of interest (Figure 20 Right).

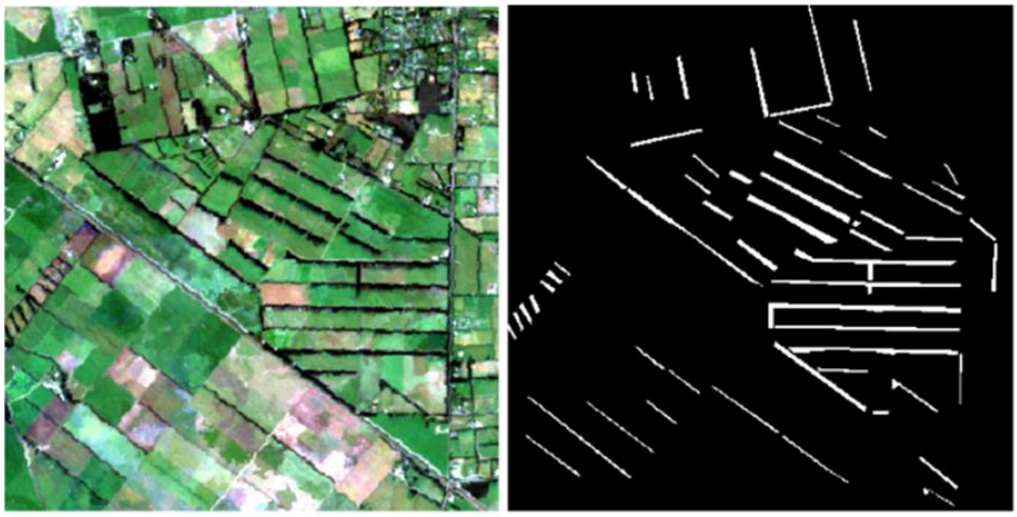

Figure 20: Sentinel-2 training image (left) with a binary raster representing known shelterbelts (right)

In this case, the binary mask layer defines what a shelterbelt (Class 1, white) should appear like and captures its inherent variation. To increase the speed of learning, graphic processor

units (GPUs) were employed in parallel. By leveraging such hardware, processing speed is an order of magnitude faster, but requires the imagery to be subdivided into smaller regions. In this case the image was divided into patches of 128 X 128 pixels and then subdivided into training and validation datasets. In total 12 patches were produced from a single training image, and from this, nine patches were used to train the AI model and three patches were ringfenced for validating model performance on different areas. Table 11 compares training and validation results using several standard statistics used in assessing AI model performance.

Table 11: Model accuracy and performance for shelterbelt detection

	Training Patches (128X128)	*Validation Patches (128X128)*
Number of images used	9	3
Time in minutes	15	1
Model loss (Error Rate %)	0.0015	0.0138
Jaccard Similarity Index (IOU)	0.9345	0.8073
Pixel based accuracy	0.9994	0.9970

To assess model outputs, a CNN AI model was trained on a single AOI and then used to predict shelterbelts on a new unknown area. Typically, to generate accurate high performing models, approximately 10% of the total area to be predicted on would be provided as correctly labelled training data. In this example, only a single tile of 16 km^2 was used as an input to the model, Figure 21 (left) showing the result of the trained model predicting shelterbelts in a confined AOI while Figure 21 (right) displays a new area in which the AI has not been exposed to, and thus completely untested. While the model output may appear to resolve the features poorly, quality control checks show the model provides a 70% accuracy in detecting shelterbelts in Canterbury Grasslands. Not a bad result when the extremely limited amount of training data that was passed to the CNN model is considered.

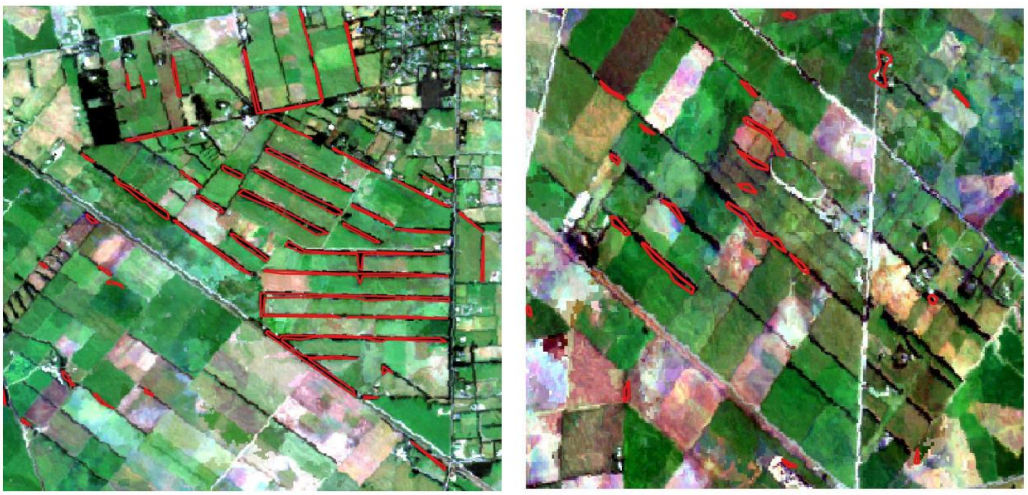

Figure 21: CNN model outputs. Training data (left) and testing/prediction (right)

6. CASE STUDY 3: GORSE/BROOM SEASONAL IDENTIFICATION

Gorse (*Ulex europaeus*) and Broom (*Cytisus scoparius*) are two competitive weed species that are similar in appearance, grow in the same environments and have a short establishment period (Figure 22). Due to this fact, the two species have been combined in LCDB. Although they appear similar, particularly at distance from the observer, both species respond considerably differently to fire. Gorse is a significant contributor to fire risk due to its ability to ignite fast and burn hot, having the potential to spread fire fast. It's area of local extent can also contribute to large areas of fire extent. This is particularly concerning in summer when the winds are hot, and conditions are dry. Broom on the other hand is difficult to burn and does not share the same fire behaviour characteristics of gorse. Because of this, it is important to distinguish between the two in relation to wildfire management.

Figure 22: Gorse orange-yellow bloom (left) and Broom bright yellow bloom (right)

Two key differences between the species may aid in differentiation and allow the use of satellite and aerial imagery to map their extent, particularly where a mix of species can be found in one area.

- Physiology. Gorse flowers in bloom have more of an orange-yellow hue than Broom, which has a brighter yellow colour. Although this may be a challenge to the human eye, it is possible to train software to delineate between the two.
- Peak blooming time. Both species typically flower in spring and have separate blooming times which occur over a window of a couple of weeks to one month. The key challenge when delineating between Gorse and Broom from satellite imagery is pinpointing the moment when one bloom ramps up and the other winds down. Therefore, the winter flowering behaviour of Gorse is particularly helpful to identify if the spring bloom contains gorse or whether it is solely Broom.

6.1. COLOUR DETECTION DELINEATION

Like exotic forestry, colour shifting using the Sentinel-Hub EO-Browser (Section 2.2.2) allows greater variability in the display of different hues of yellow. This method has been successfully applied to explore the temporal change in yellow flowers in an AOI in the hills above Akaroa in Canterbury. Figure 23 shows a time sequence that shows the progression from dark yellow on 3rd October through to bright yellow on 27th November. These images show how the extent of yellow changes in conjunction with the shade of yellow supporting the different blooming time of Gorse and Broom.

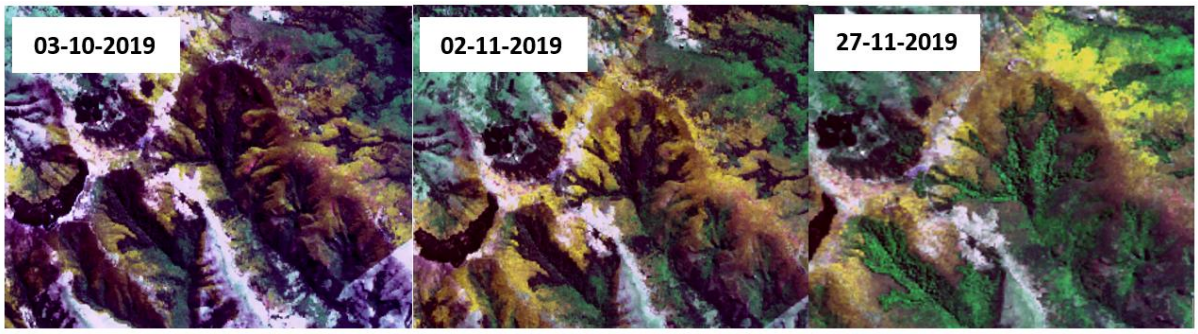

Figure 23: Yellow flower bloom over time

Assuming the blooming time of Broom in Canterbury to be November, a test was done comparing areas identified by Environment Canterbury (ECan) (Figure 24) with Sentinel-2 imagery (Figure 25). The ECan features are mostly correct in their location when compared with the bright yellow blooms in the satellite imagery.

Figure 24: Areas identified by ECan as being predominantly broom. Purple – dominant, Orange – common, Blue – frequent

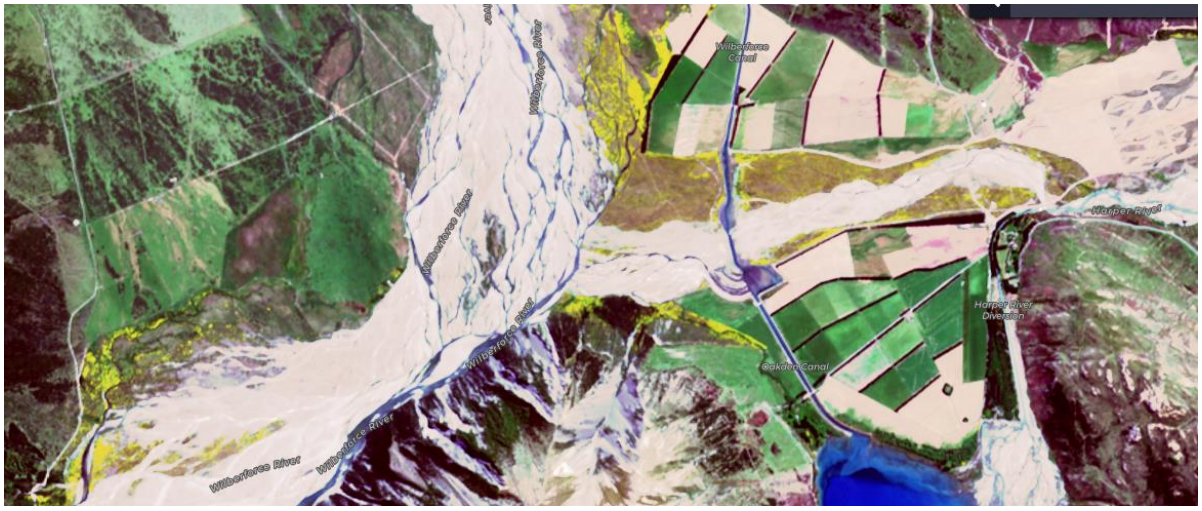

Figure 25: Sentinel-2 satellite imagery from 2019 showing a bright yellow bloom in mid-late November.

A further examination into the LCDB2 classification in relation to gorse has occurred in Taupo (Figure 26), where a side-by-side comparison of the LCDB2 gorse classification and a colour shifted satellite image from mid-late November 2017 was undertaken. It appears that there is minimal crossover between the two, likely due to the difference in analysis times, and that Gorse in this area is no longer correct. Additionally, depending on the acquisition date of imagery that was used to create LCDB2, it also may not be Gorse. As shown in the Canterbury examples above, Broom also flowers in mid-late November and has a similar bright yellow flower to Gorse.

Figure 26: LCDB2 classified gorse and broom in yellow (left), Satellite imagery (November 2017) showing yellow bloom (right)

6.2. TEMPORAL DETECTION DELINEATION

Given that Gorse and Broom have similar coloured flowers, this may cause difficulties when attempting to delineate between the two in a mixed species setting. The use of a single date imagery source, even one of high resolution (i.e. Worldview 3), may not be adequate in providing an AI algorithm a chance to successfully identify a feature/species of choice. Given that the Sentinel-2 imagery used in this report is of medium spatial (i.e. 10 m/px), but relatively high temporal resolution (five-day revisit time), a different approach may be needed.

Such an alternative to finding the colour difference between blooms is to employ the temporal component of flowering to determine if Gorse is present. Thus, extending the time component from a couple of weeks to several months may increase the probability of separating Gorse from Broom.

The blooming period for Gorse is generally longer and earlier to that of Broom, typically beginning in mid-late winter and extending through spring and summer. In contrast, Broom tends to only flower during mid-late spring. Although the winter bloom of Gorse may be less dramatic than the spring bloom, it is still possible to detect its presence (Figure 27).

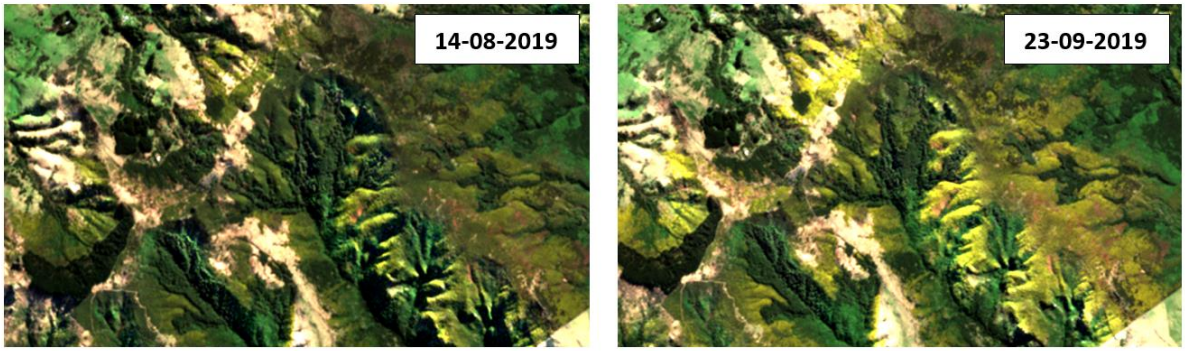

Figure 27: Gorse bloom in winter (left) and spring (right). Note that these images have a different colour setting than those in Figure 23.

To employ such a method would require image processing software and a customised yellow spectrum. Additionally, it would also take a month, or at least two weeks of images to determine if gorse or broom is present and the degree of change in the coverage. It would also be possible to determine the degree of change of average colour of each pixel to help detect the period where the bloom goes from an orange yellow to a brighter yellow to assist with species delineation.

An example of this application would be if yellow is present only in November, its likely to be broom. But if yellow present from late August to late November, its likely gorse is present. The colour change analysis could assist in delineating where gorse and broom are present. Unfortunately, given that building custom colour stretches, waiting for the correct period and the number of images required is particularly time intensive, therefore it may only be financially viable to undertake this once a year.

6.3. IMAGE CLASSIFICATION

To apply a machine learning methodology to the problem of Gorse/Broom detection and delineation, an AOI was chosen in the hills on either side of Akaroa Harbour. Sentinel-2 true colour imagery was collected for the period October to November where a clear shift in the extent of yellow vegetation was observed. The open-source image processing application Fiji (https://imagej.net/Fiji), was used to build a training dataset for the earlier part of the Gorse blooming period (Early October) and applied to a second time-slice in which Broom was likely to be flowering (November).

The Sentinel-2 true colour imagery for the October 2017 period (Figure 28) shows Gorse as having a subdued orange/yellow colour and typically being restricted to the higher elevation ridgetops and their associated slopes. In contrast, in the November imagery (Figure 29), the same vegetation appears far brighter and has a smaller extent. While this is likely due to the differing blooming periods and species composition between the Gorse and Broom, it may also be related to hue and gamma differences between the two images.

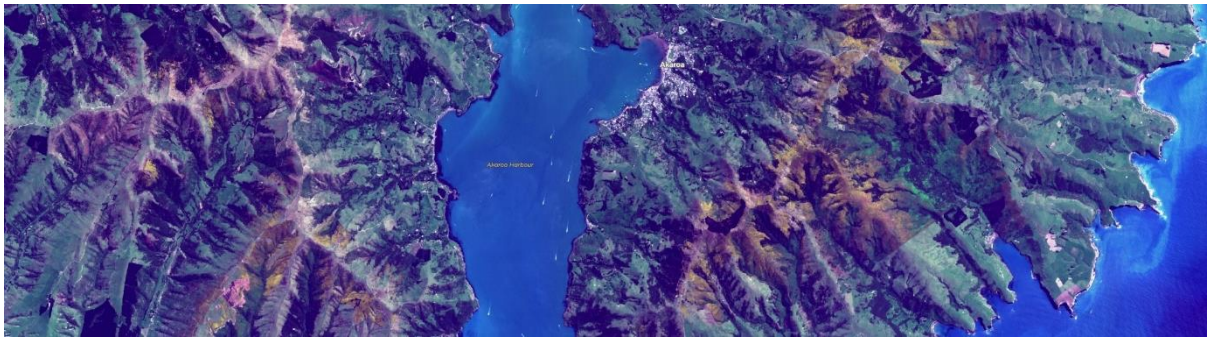

Figure 28: Sentinel-2 imagery from October 2017.

Figure 29: Sentinel-2 imagery from November 2017.

Using the Fiji software, key areas from the above imagery were extracted for use as training data. The classified results for each date were post processed to reduce any classification noise and are shown in Figures 30 and 31.

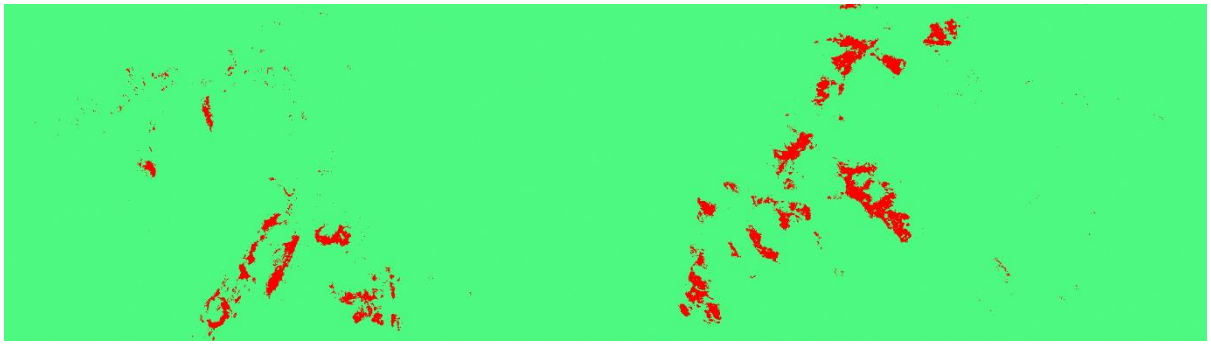

Figure 30: Gorse areas identified in October imagery using the Fiji classifier.

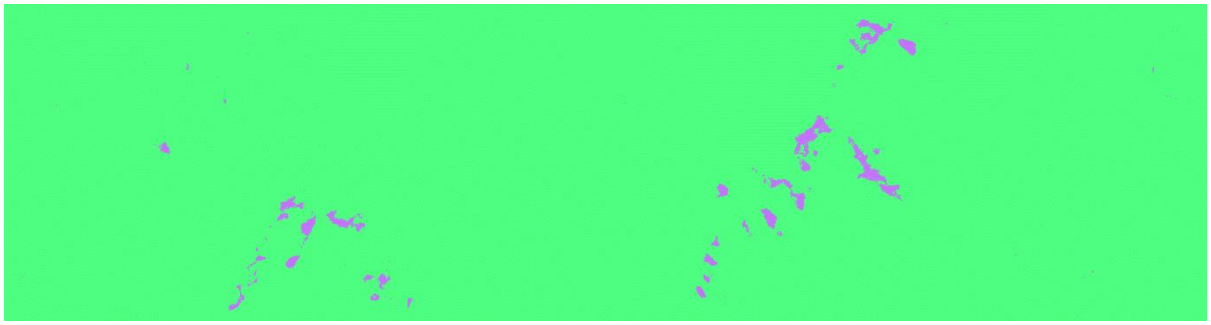

Figure 31: Gorse areas identified in November imagery using the Fiji classifier.

We have shown that by using a range of techniques the separation of Gorse vs Broom is possible using Sentinel-2 data. Even with its lower resolution, the short revisit time of the satellites allows the temporal nature of blooming times between the two species to be quantified.

7. CASE STUDY 4: URBAN EXPANSION

A key part of assessing the threat that wildfire poses to people and property is understanding the expansion of urban or peri-urban areas into the surrounding rural area. With changes to city limits and shifting population centres, the potential for proximity of residential and commercial properties to extensive areas of vegetation has increased. This is especially important when considering the risk posed by shelterbelts and windbreaks, commonly found in farm settings, as a fire corridor though the establishment of a continuous fuel pathway. Given these concerns, developing a methodology to enhance LCDB5, which is based on 2018 data, will provide a clearer picture of potential risk to properties along the rural-urban interface.

To examine the changes in urban and commercial expansion, Sentinel-2 imagery was obtained for January 2016 and 2020. Christchurch was chosen due to its extreme post-earthquake population shift, in which residents in the affected Eastern and Central suburbs have relocated to Western and Northern areas.

Imagery was created using the red and SWIRs band:

$$FCSWIR = R_{(B12)}\ G_{(B11)}\ B_{(B4)}$$

Where Red = SWIR2 (Band 12), Green = SWIR 1 (Band 11) and Blue = Red (Band 4). The use of such a false colour band combination highlights the differences between the urban and rural areas between the two years (Figure 32).

Figure 32: Sentinel-2 false imagery for Christchurch city in 2016 (Left) and 2020 (Right).

An initial observation of the imagery shows the city as being comprised of two distinct pixel textures and colours.

- **Type 1**. Light pixels. Located in regions with a high proportion of larger industrial and commercial warehouses and buildings. The large roofs,

typically galvanised or painted white, provide a highly reflective surface to all wavelengths. The central commercial corridor running east / west across the city is particularly obvious in Figure 32.

- **Type 2**. Grey pixels. These represent the highest proportion of the city and are caused by a mosaic of residential dwellings and their associated gardens. Compared to that of the commercial zone, the different spectral responses from a range of vegetation, roof size and building material produce a more textured appearance in the imagery. Additionally, due to the smaller size of residential building compared to the 10 m pixel size resolved by the Sentinel-2 imagery, the reflected wavelengths are a mix of building and vegetation.

Using the false colour imagery, a relatively small number of areas (n=15) representing the above two types were digitised and provided to a Support Vector Machines (SVM) classification algorithm as training data. As the identification of urban areas is a binary problem (absence vs presence), the training data only needed to represent the variation observed.

SVM excels in binary segmentation and thus the relatively simple set of input pixel types and limited training data have produced the outputs shown in Figure 33.

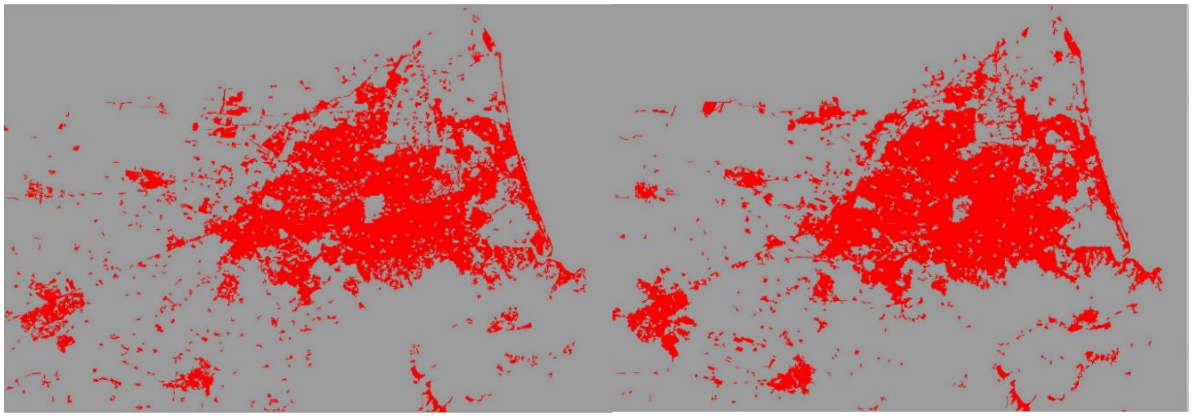

Figure 33: Urban areas in 2016 (Left) and 2020 (Right) from the SVM model.

Unsurprisingly the model shows an expansion of areas now classed as urban into the western formally rural areas, particularly around the towns of Rolleston, West Melton, and Lincoln. Both commercial/industrial and residential areas have been well segmented from the surrounding rural and peri-rural area. If the difference between the 2016 and 2020 data is calculated, the result is the areas of absolute change (Figure 34). Unfortunately, as can be seen, some areas of non-urban areas have been highlighted (i.e. wastewater ponds to the east).

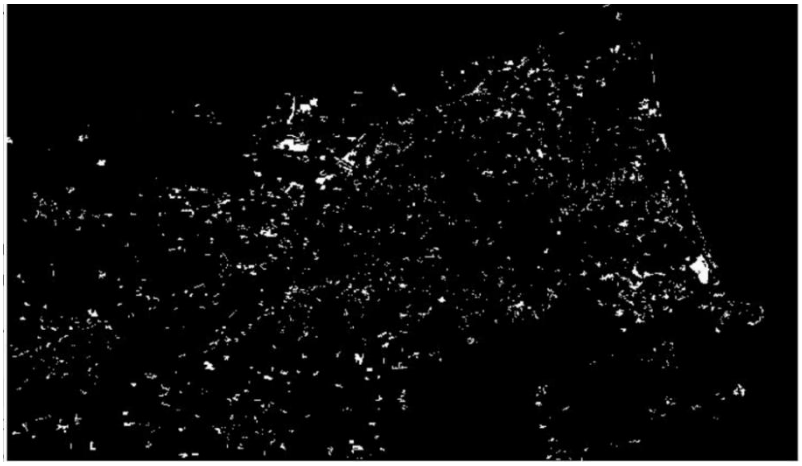

Figure 34: Binary output showing areas of change from 2016 to 2020.

8. CASE STUDY 5: WATER BODY DETECTION

While obviously not a wildfire fuel source, water availability is a key resource when considering rural fire operations in remote locations. This is especially pertinent to helicopter operations that use monsoon buckets and require access to open water bodies during wildfire outbreaks. Therefore, identifying and providing an up-to date dataset of suitable locations to collect or extract water is a key component of any wildfire response database.

To explore the AI detection of water features, an AOI was defined that covered approximately a quarter of the Canterbury region. Within this area were located a range of surface water types such as lakes, ponds, reservoirs, lagoons, and rivers, all of which play an important role in wildfire management either as a water resource or a physical barrier to fire spread. To assess the use of AI in water detection 10 m resolution Sentinel-2 true-colour imagery was acquired from January 2016 to June 2019 and filtered to ensure less than 10% cloud cover (Figure 35).

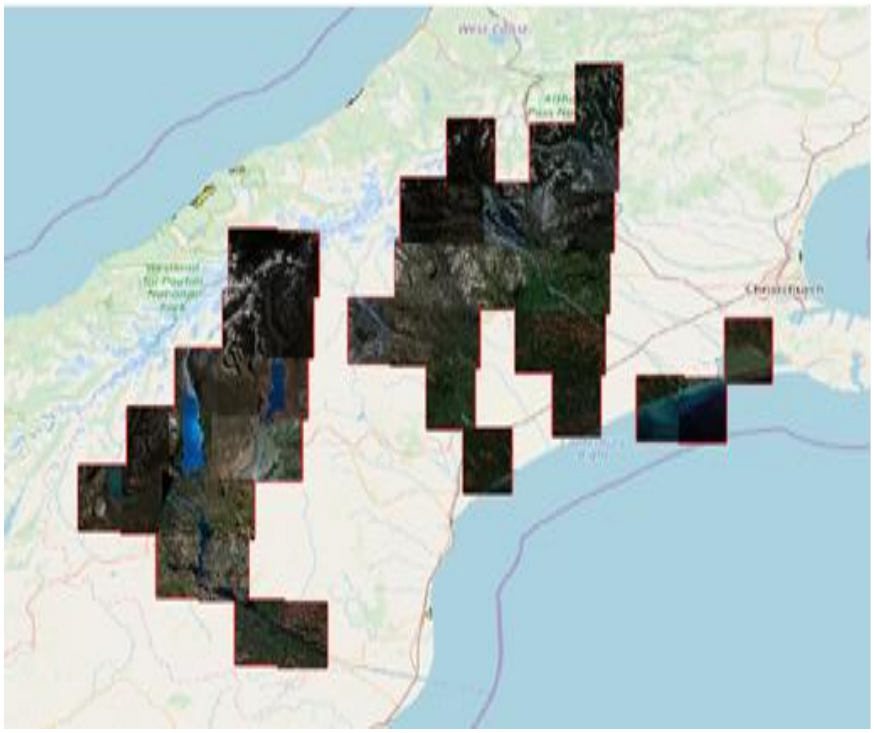

Figure 35: Sentinel-2 imagery used in the Canterbury region to assess water coverage.

Additionally, to generate the required training data, the 2018 LINZ water body dataset was used to define areas of surface water.

Using the Sentinel-2 imagery, a relatively standard band combination was used to enhance the detection of surface water, that being the Normalised Difference Wetness Index (NDWI) which is derived from the relative differences between the green (Band 3) and near infrared (Band 8).

For each image in the dataset, a label needs to be generated in a binary format which represents the actual water region. To do this the NDWI has a threshold value applied to extract all pixels that represent water and reduce pixel noise that might be observed within the dataset. Finally, to further clean the NDWI data, a range of negative data is applied as a masking function. Non-water features such as roads, buildings, and forests, are obtained from sources such as LINZ and Open Street Maps (https://www.openstreetmap.org/) and used to ensure accuracy of the training data (Figure 36).

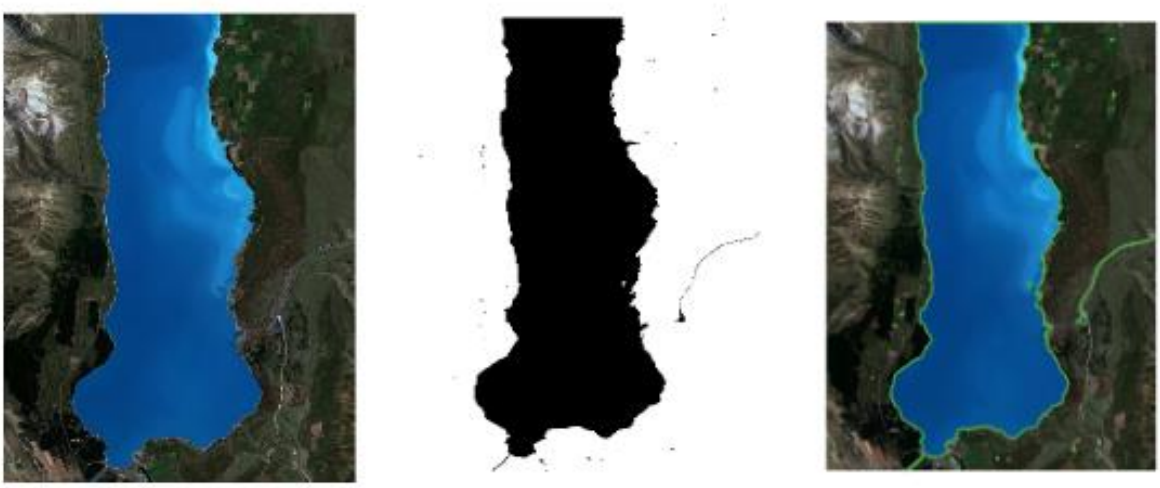

Figure 36: An example of steps required to produce training data. Sentinel-2 true colour imagery of Lake Pukaki (left), thresholded NDWI (centre) and vector polygon outputs (right, green lines).

Like that of the shelterbelt example (Section 5), images are subdivided to allow the use of GPU acceleration. 60 Sentinel-2 training images are subdivided into 16000 patches (128x128 pixels), and further subsampled, with ~25% (n=4000) held back for use in validation.

Convolution Neural Network (CNN) algorithms are trained on, and then tested, using several band combinations to assess for accuracy and model performance.

- Three bands. True colour (RGB) only.
- Four bands. True colour (RGB) + merged greyscale band.
- Four bands. True colour (RGB) + NDWI band.

The outcome of these tests produces several key parameters that are used in the tuning of the final model and by doing some QA/QC on the training and validation results, we can say that the model is >85% accurate (Table 12).

Table 12: Typical output of CNN training vs validation vs testing model.

	Training	*Validation*	*Testing*
Number of arrays	12066	4021	2681
Number of images	45	15	10
Model loss (%)	0.0098	0.0090	-
Jaccard similarity (IOU)	0.8988	0.9022	-

Final model outputs for the unknown testing areas are shown for lakes (Figure 37), braided rivers (Figure 38) and a mixture of water body types including alpine tarns and ponds (Figure 39).

Figure 37: Sentinel-2 true colour imagery (left) and the AI outputs (right) for Lake Ohau in South Canterbury. Note the lack of definition between lakes Middleton and Ohau (green box) likely due to incomplete classification in the AI processing pipeline.

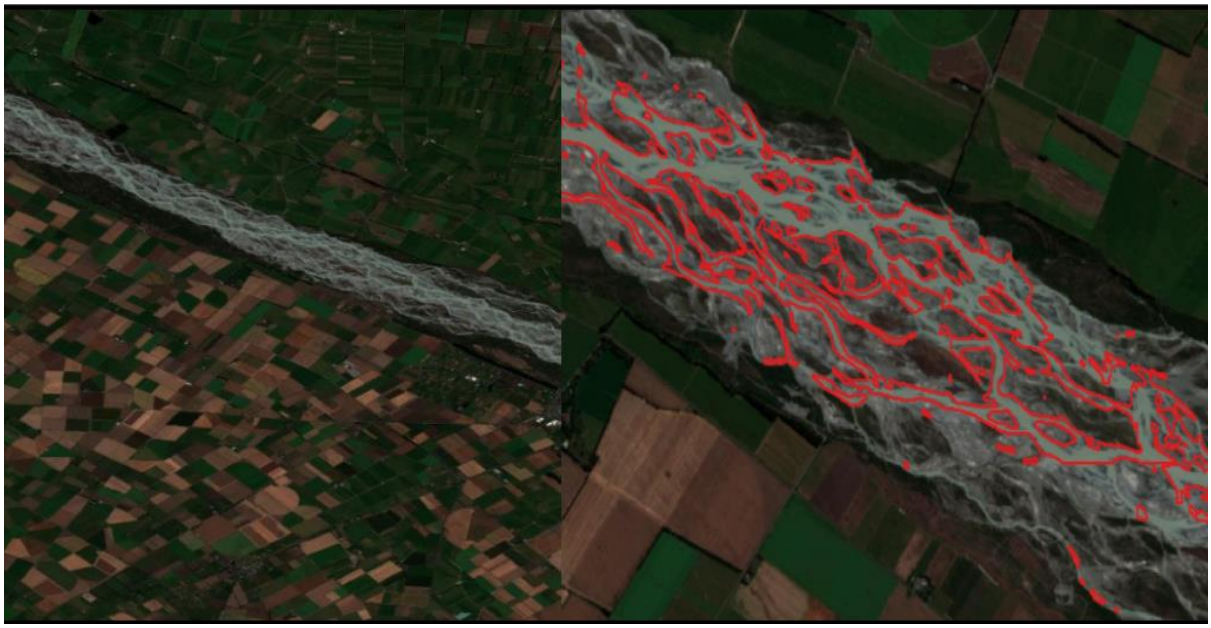

Figure 38: Sentinel-2 true colour imagery (left) and magnified view of the AI outputs (right) for the Rakaia River.

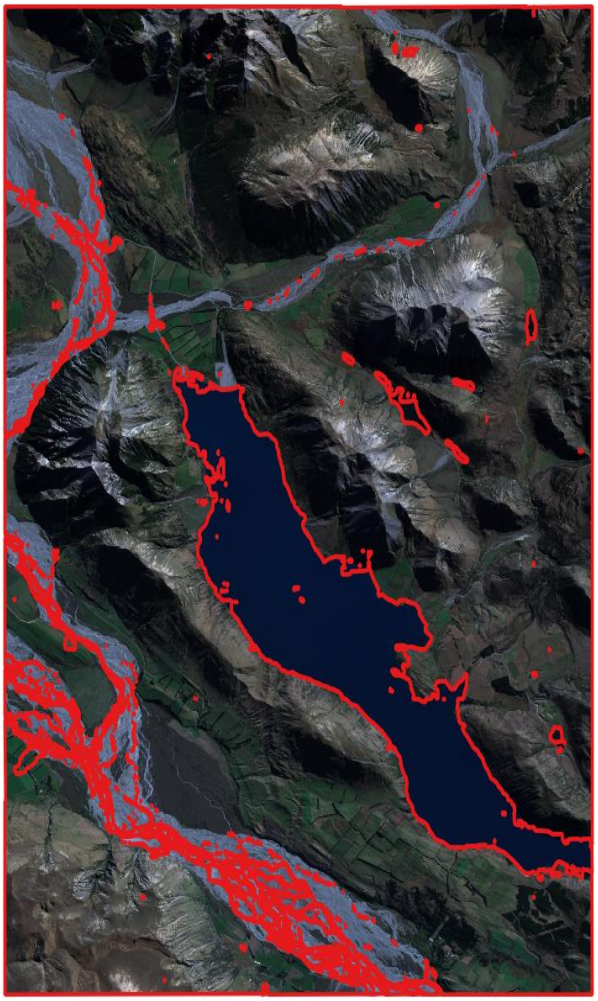

Figure 39: Outputs from the CNN model when applied to the Lake Coleridge and upper Rakaia River area.

Results from this example show that the combination of CNN machine learning, and multispectral Sentinel-2 imagery can be used to extract areas of surface water with a fairly high level of accuracy. As always in small case study investigations like this example, additional steps could be added to increase accuracy and processing speed, while decreasing model error. In particular:

- More training data.
- Tuning of Hyperparameters to increase the model accuracy.
- The addition of new imagery like thermal (Landsat 8) and other spectral bands (Sentinel-2) will increase the amount of input data pixels provided to the model and thus will help deep learning models to identify new features.
- Adding more post processing to filter/remove noise from output predictions.
- Investigate methods to improve class imbalances (i.e. the ratio between water and non-water pixels).

9. CONCLUSION

The findings presented in this report show, albeit at a relatively basic level, that the use of machine learning and artificial intelligence algorithms can be used to identify and isolate key wildfire fuel types. As well as a deep dive on the class differences between LCDBv2 and v5, our results find:

- The systematic errors observed between previous and current versions of LCDB may make the use of future releases problematic for the differentiation of wildfire fuel classes and associated fire behaviour modelling.
- That given the correct amount and type of training data, machine-learning and artificial intelligence models can be used to detect a range of expanded-fuel classes, not current in LCDB5 and certainly not in LCDB2.
- Sentinel-2 at 10 m/px provides an adequate spatial resolution for most purposes. Only shelterbelts with a width less than 10 m may be problematic.
- Using colour and temporal shifting techniques, gorse and broom may be able to be separated at some level using their differing flower colour and blooming times.
- Using aerial imagery, several exotic forestry classes can be identified.
    - Cleared areas (i.e. slash and cutover).
    - Different age classes.
- Changes can be relatively easy to observe using several Sentinel-2 products. In cases where this is not possible, applying colour shifting techniques may increase the accuracy in the identification of native vs exotic forestry stands.
- False colour imagery provides a solid platform for the detection of urban areas and thus the encroachment into rural areas.
- Sentinel-2 NDWI data can be used to identify water features such as lakes and rivers throughout Canterbury.

9.1. FUTURE RESEARCH DIRECTIONS

Given that this research only touches on a limited number of fuel types, several areas where expanded work may be a benefit have been recognised.

- **More targeted work on fuel types**. While good progress was made on recognising the extent of gorse vs broom, other mixed fuel types would also benefit from a closer view.
- **Grasslands.** New Zealand has a variety of grass types, from dry alpine tussocks and wet marshlands. Currently most of these differing fuel types are clustered together into the ubiquitous LCDB “Grasslands” class which poses problems for determining fire behaviour. The identification of grassland extent and species is also important when considering the encroachment of urban areas.
- **Exotic vs native forestry.** While the identification of exotic plantations was covered at a simple level, a more in-depth investigation would allow the development of a more robust AI model. If more forestry companies could

supply GIS data for the extent and species of plantations, this could be used as training data to drive a far more accurate model using satellite imagery.

- **Testing.** Producing a small AOI with the AI generated features from this project and integrating them into LCDB5.
- **Full AI model**. For this work, the discussed fuel types were treated as their own discrete entity, each having a range of imagery, processing, and algorithm types. Yet this is not the case as all these fuel types are a patchwork across the New Zealand landscape. Now with our understanding of how machine learning, and AI models react to the training data and the requirements needed to produce more accurate models, a proof-of-concept methodology using a single multiclassification AI model could be developed. This work could be done with a local view, being run on inhouse machines, or the initial start of a cloud-based solution (see below).

9.2. IMPLEMENTATION

Given the final option presented above, such an AI driven classification pipeline could be imagined in several ways, depending on the required timeliness of data delivery and update frequency. While estimated costs have been added, final costing may vary considerably based on the extent of the AOI being processed (All prices in NZD).

- **Timed release.** In this scenario FENZ would subcontract the production of an augmented LCDB that adds/updates key vegetation fuel types as specified. This would be produced on local machines and would not require any cloud-based technologies (i.e. AWS and Azure). This dataset would not be the latest snapshot of vegetation fuel types but be far more accurate than the currently employed version of LCDB. The frequency of releases could be biannually or annually as required.

  Estimated cost per release: $20-40k.

- **On demand (ad-hoc)** – local computing. A reactive approach would be that a targeted dataset, using an AOI defined by an active event, is produced when required. An advantage is that the latest imagery can be used and thus the dataset is the most update (within the five-day revisit time of Sentinel-2). This could also be combined with high resolution commercial imagery if required.

  Estimated cost per event: $5-15K.

- **On demand** – cloud computing. Like the above, but the entire process is based within a cloud-based infrastructure. In this situation, FENZ could have complete control of the process and outputs would be automatically generated on a weekly basis, or manually requested in the event of an active wildfire. This is a proactive approach where the latest data is constantly being produced.

  Estimated cost for development and setup: $100-200k.

For all these scenarios, a web portal for operational and management purposes using this data can also be produced. The ability to provide “boots on the ground” firefighting personnel with mobile accessible data may be a powerful tool in the fight against wildfires.